THESIS

LIBRARY
Michigan State
University

MICHIGAN STATE LIBRARIES
3 1293 01801 7081

This is to certify that the

thesis entitled

SYNTHESIS OF GROUP 4 METAL β-DIKETIMINE COMPLEXES

presented by

William J. Scanlon IV

has been accepted towards fulfillment
of the requirements for

Masters degree in Chemistry

Major professor

Date 12/17/98

O-7639

MSU is an Affirmative Action/Equal Opportunity Institution

PLACE IN RETURN BOX to remove this checkout from your record.
TO AVOID FINES return on or before date due.
MAY BE RECALLED with earlier due date if requested.

DATE DUE	DATE DUE	DATE DUE

1/98 c:/CIRC/DateDue.p65-p.14

SYNTHESIS OF GROUP 4 METAL β-DIKETIMINE COMPLEXES

By

William J. Scanlon IV

A THESIS

Submitted to
Michigan State University
in partial fulfillment of the requirements
for the degree of

MASTER OF SCIENCE

Department of Chemistry

1998

ABSTRACT

SYNTHESIS OF GROUP 4 METAL β-DIKETIMINE COMPLEXES

By

William J. Scanlon IV

Controlling stereochemistry in synthesis is important in many industries. Efficient methods of separating readily available racemic modifications into their respective enantiomers are in high demand. This thesis chronicles initial syntheses of a family of group 4 transition metal compounds stabilized by β-diketimine ligands, which are precursors to catalysts for use in kinetic resolution via polymerization.

Reaction of TTPH (TTP = 2-p-tolylamino-4-p-tolylimino-2-pentene) with $M(NMe_2)_4$ (M = Zr, Ti) affords $(TTP)M(NMe_2)_3$ and $(TTP)_2Zr(NMe_2)_2$. $(TTP)Zr(NMe_2)_3$ reacts further with *p*-toluidine to form the imine $(TTP)Zr(=NC_6H_4CH_3)(NMe_2)$ (^1H NMR). TTPH reacts with $Zr(CH_2C_6H_6)_4$ to give $(TTP)Zr(CH_2Ph)_3$, which undergoes ortho-metallation with elimination of toluene via direct σ-bond metathesis to form $(\eta^3$–$MeC(NC_7H_6)CHC(N$–*p*–$Tol)Me)Zr(\eta^2$–$CH_2Ph)(\eta^1$–$CH_2Ph)$ ((TTP*)$Zr(CH_2Ph)_2$). DDPH(HCl) (DDPH = 2-(2,6-diisopropyl)phenylamino-4-(2,6-diisopropyl)phenylimino-2-pentene) reacts with $Zr(NMe_2)_4$ to yield $(DDP)ZrCl(NMe_2)_2$.

Metathesis reactions of Li(TTP) and Li(DDP) with group 4 tetrachlorides produce $LMCl_3$ (L = TTP, DDP and M = Zr, Ti,) and L_2MCl_2 (L = TTP, M = Zr).

All compounds were characterized using ^1H and ^{13}C-NMR and in many cases single crystal x-ray studies and elemental analysis.

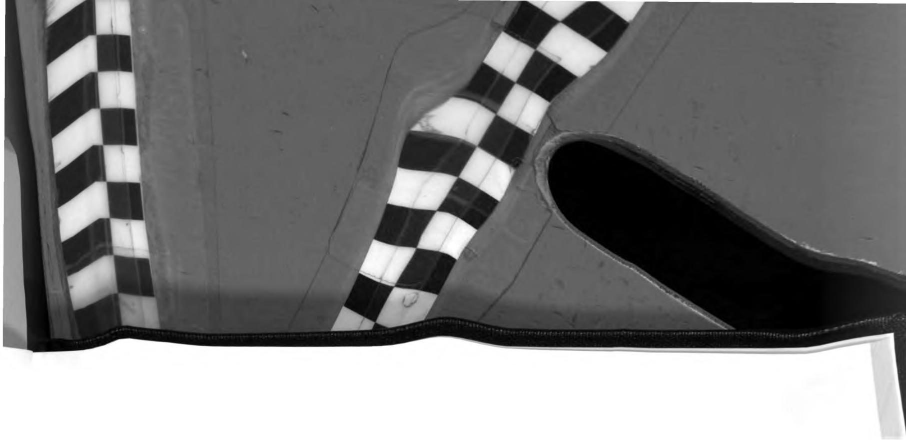

To my old friend, Herschel Schmoykel Krustofsky

ACKNOWLEDGEMENTS

First, I would like to thank Dr. Mitch Smith III for his sometimes sarcastic, often humorous and always honest and helpful insight and guidance.

Second, I'd like thank Carl Iverson, Dean Lantero, Baixin Qian and the rest of the Smith group, whose assistance in my Graduate School experience was priceless.

Lastly, I'd like to thank Pete LeBaron, Paul Szalay and Randy Hicks for countless hours of pointless pontification and intellectually insulting conversations.

TABLE OF CONTENTS

LIST OF TABLES

LIST OF FIGURES

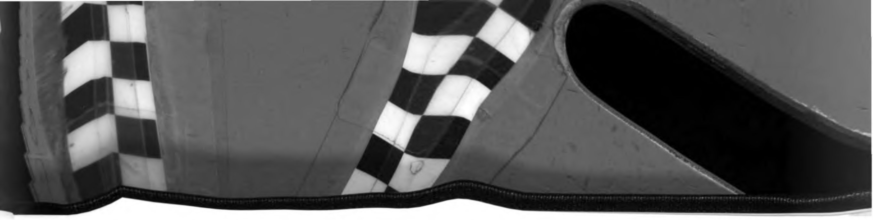

LIST OF ABBREVIATIONS

TPH	4-p-toluidino-pent-3-en-2-one
TTPH	2-p-tolylamino-4-p-tolylimino-2-pentene
(TTP*)Zr(CH_2Ph)$_2$	(η^3–MeC(NC_7H_6)CHC(N–*p*–Tol)Me)Zr(η^2–CH_2Ph)(η^1–CH_2Ph)
TMPH	4-(2,4,6-trimethyl-anilino)-pent-3-en-2-one
DPH	4-(2,6-diisopropyl-anilino)-pent-3-en-2-one
DPPH	2-(2,6-diisopropylphenylamino)-4-(2,6-diisopropylphenylimino)-2-pentene
DTPH	2-(dimethylamino-4-(4-tolylimino)-2-pentene

CHAPTER 1

INTRODUCTION

Methods of Asymmetric Synthesis

Obtaining optically pure reaction products (asymmetric synthesis) is often paramount in fully realizing a compound's practical utility. For example, pharmaceutical compounds commonly have one active enantiomer and another that is inert, deactivating, or even toxic.[1] As a result, enantiospecific synthesis has evolved into an important synthetic discipline.

There are basically two methods used to synthesize chiral molecules: kinetic resolution and enantioselective synthesis from prochiral substrates (Figure 1). In kinetic resolution, a chiral auxiliary is added to a racemic modification. The auxiliary selectively reacts with one enantiomer leaving the other behind. This method is convenient because racemic modifications are readily available. The inherent downside to kinetic resolution is consumption of half of the starting material (ie., maximum yield is 50%). Direct enantioselective synthesis does not have this problem. This method relies on interaction between a chiral auxiliary and a prochiral substrate to produce only one enantiomer. In this way, all of the starting material (in theory) can be converted to chiral product. This approach requires that functionality be introduced with high regio and stereoselectivity, whereas the desired funtional group is already in place in kinetic resolution schemes.

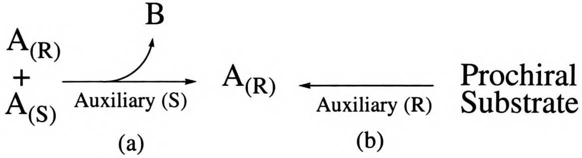

Figure 1 (a) Kinetic Resolution and (b) Enantioselection

Both of these methods can proceed stoichiometrically or catalytically. Catalytic reactions have one large advantage over using stoichiometric reagents, namely stoichiometric amounts of chiral auxiliary are not required. For these reasons and others, asymmetric catalysis has received considerable attention in recent years.[2-4]

Nature employs catalysts (such as enzymes or entire cells) that perform asymmetric catalysis with a sublime mastery. These biocatalysts have been "domesticated" by chemists and used for synthetic processes.[2] For instance, pig liver esterase (PLE) is an enzyme that hydrolyzes the various of esters ingested by pigs. It is the most widely used esterase in enzymatic asymmetric synthesis, because it accepts such a wide range of substrates. PLE is usually utilized in enantioselective synthesis via the '*meso* trick'. As exemplified in Figure 2 (bottom), PLE selectively hydrolyzes one of the esters in a *meso* diester compound.[5] The resulting chiral compound is recovered in high yield and high enantiomeric purity. Using PLE, this approach has been extended to kinetic resolution. In Figure 2 (top), PLE is added to a racemic modification of chiral esters.[6] It selectively hydrolyzes one of the enantiomers, which can be recovered in high yield and high enantiomeric excess. The high yields and excellent enantiomeric excesses

enhance the appeal of PLE catalysis, but syntheses that exploit these systems are sometimes limited.

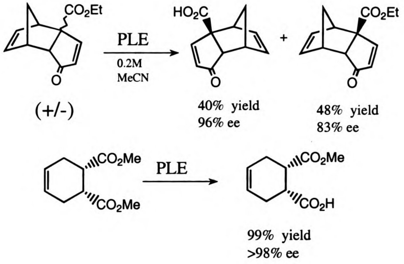

Figure 2 PLE 'meso' Trick (bottom) and Kinetic Resolution Via Hydrolysis (top)

In recent years, inorganic systems have begun to rival biological ones in their utility. Noteworthy advantages of inorganic metal asymmetric catalysts over biological catalysts are as follows: (i) metals can perform reactions natural systems will not; (ii) chiral metal catalysts can be easily alterable through ligand modifications; (iii) metal catalysts can be designed to withstand non-biological environments; and (iv) metal catalysts can accept a wider variety of substrates than biocatalysts.[7]

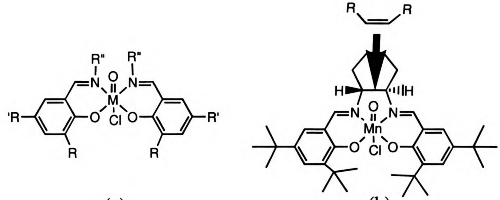

(a) (b)

Figure 3 (a) (salen)MCl (b) Olefin Approach

Jacobsen has recently reported enantioselective epoxidation of *cis*-olefins[8] and kinetic resolution of terminal epoxides via catalytic hydrolysis,[9] using metal complexes. In the case of enantioselective epoxidation, changes in the enantiomeric excesses with variations of the R, R' and R" groups were observed (Figure 3(a)). The highest enantioselectivity was obtained when the steric properties were adjusted such that olefin interaction with the dissymmetric portion of the ligand was maximized (Figure 3(b)). These results demonstrate the importance of controlling the steric properties of an asymmetric catalyst. The simple reaction mechanism shown in Figure 4 was proposed for epoxidation. It suggests that addition of an alkene (ex. *cis*-olefin substrate) to the oxo moiety generates a radical intermediate. In this intermediate, the alkyl group can collapse (forming the cis isomer) or rotate and collapse (forming the trans isomer).

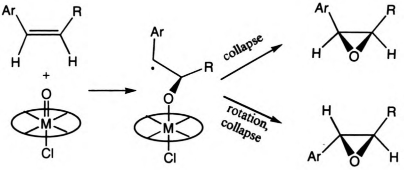

Figure 4 Jacobsen Mechanism

Jacobsen also demonstrated the dramatic effects of catalyst electronics on asymmetric synthesis (at least in the case of epoxidation).[10] By varying the R' group from electron donating (ie., R' = OCH_3) to electron withdrawing (ie., R' = NO_2), a change in the enantioselectivity of the catalyst was observed. The electron donating groups were found to increase the enantioselectivity. The proposed explanation presumes that the high-valent (salen)Mn(IV)O-olefin intermediate influences the stereochemistry of the epoxide in accord with the Hammond postulate in the following way. The electron donating groups stabilize the intermediate, making it a milder oxidant so that the oxygen to alkene transfer proceeds via a more product-like transition state. At the origin of the reaction coordinate, the reactants do not interact at all. Therefore, a higher degree of stereochemical communication might be expected in the later transition state. The electron withdrawing substituents are expected to destabilize the intermediate, making it a more reactive oxidant. Here a more reactant like transition state might be expected with poorer stereochemical communication.

This example emphasizes the importance of being able to control the electronic and steric properties of a catalyst. Transition metal compounds have long been used to

catalyze several types of reactions including polymerizations and organic syntheses such as hydroformylations, hydrogenations, hydrocyanations and hydroborations.[11] In recent years, they have become important tools in asymmetric syntheses. Their ability to accommodate various ancillary ligand sets makes them ideal to obtain the electronic and steric tuning requirements necessary to design efficient enantioselective catalysts.

A Word on Polymers and the Importance of Stereochemical Control

The importance of polymers is evident in almost every facet of daily life. For example, polypeptides are important natural polymers composed by linking together many amino acids. They are present in enzymes, and fill many other important roles in natural biochemistry. DNA is another example of a very important natural polymer. Natural polymers such as wool and silk, which are also polypeptides, have been used for thousands of years.

In the twentieth century, chemists have developed numerous methods to synthesize unnatural polymers. These polymers are used in more wide and varied applications than any other class of chemical. Polymers are employed as fibers, plastics, or elastomers. Fibrous polymers are strong, deformation resistant substances used in the manufacture of clothing and ropes. Plastic polymers are classified as rigid plastics and flexible plastics. Rigid plastics are hard, non-flexible materials that find applications ranging from appliance housings to hardhats. Flexible plastics, conversely, are softer, much more pliable substances. They find use as packaging films. Elastomers are extremely flexible polymers that return to their original shape and size after being stretched a great deal.[12]

The properties (hardness, flexibility, melting points, elasticity, etc.) of polymers depend on several variables including the identity of the monomers, the molecular mass of the polymer and the amount of branching in the polymer. Some monomers contain stereocenters or have the potential to form stereocenters upon polymerization. In such cases, orientation of relative stereocenters can have a marked effect on the properties of the polymer.

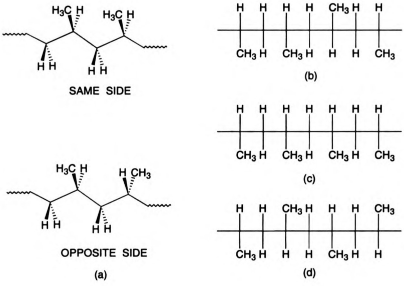

Figure 5 Tacticity in Polypropylene (a) Possible Configurations (b) Atactic (c) Isotactic (d) Syndiotactic

Polypropylene is one of the simplest examples of a prochiral monomer. During polymerization, the methyl group can adopt syn or anti configurations with respect to the previous stereocenter (Figure 5(a)). The stereoregularity is termed tacticity. Three different tacticities are possible. In the first situation, the configurations of the stereocenters are distributed randomly (Figure 5(b)). The polymer is then said to be **atactic**. In the second case, consecutive stereocenters have identical configurations (ie. R groups are on the same side (Figure 5(c))). These polymers are termed **isotactic**. In the

last case, polymers have consecutive stereocenters with repetitive *alternating* configurations (ie. each R group is opposite of the previous (and subsequent)(Figure 5(d))) and a **syndiotactic** polymer results.

Atactic polymers have difficulty in packing efficiently into a crystal lattice, because of their irregular configurations. As a result, they tend to be amorphous (noncrystalline), soft ('tacky') substances with little or no physical strength. Atactic polymers find few applications in industry. On the other hand, isotactic and syndiotactic polymers tend to pack well in crystal lattices, because their regular structures allow for closer interaction of the polymer chains. The resulting polymers are highly crystalline substances that are physically robust and display good resistance to solvents and chemicals. Isotactic and syndiotactic polymers have wide-ranging industrial applications.

Olefin Polymerization Catalysts Supported by Cyclopentadienyl Ligands

Ziegler-Natta catalysts (generally consisting of a Group 3-8 transition metal with a Group 1, 2 or 13 organometallic) have been very successful in facilitating low temperature-low pressure polymerizations. Some early, Ziegler-Natta catalysts gave stereoregular polymers. For example, Natta found that the polymerization of propylene using $TiCl_4/Et_2AlCl$ gave a highly isotactic polymer.[13] These early Ziegler-Natta catalysts were heterogeneous. In such systems, the control of the polymer stereochemistry is derived from the chirality of the crystal lattice.[12] Active sites are thought to be located at defects on the crystal surface. Modifying the chirality of the crystal or adjusting the active site is virtually impossible. Thus, heterogenous catalysts offer little real control of polymer stereochemistry.

Cyclopentadienyl (Cp) organometallic compounds of the type Cp_2MX_2 (when activated with methylaluminoxane (MAO) or other Lewis acids ($[Ph_3C][B(C_6F_5)_4]$ or $B(C_6F_5)_3$) have become extensively used as homogeneous Ziegler-Natta catalysts. Polymerization in these species proceeds via olefin coordination and insertion of a cationic transition metal species.[14] The cation is generated *in situ* when MAO is used as a cocatalyst. $[Cp_2MR^+][BAr_4^-]$, however, can be synthesized upon reaction of Cp_2MR_2 with $[Ph_3C][B(C_6F_5)_4]$ or $B(C_6F_5)_3$ and then used in polymerization. Either way, the formation of a cationic species appears to be important to catalytic activity.[15]

Some of these homogeneous systems have shown stereoselectivity. The $(Cp)_2Ti(Ph)_2$ / MAO system, for example, produces isotactic polypropylene.[16] This system is unusual, as most stereoselective catalysts are chiral molecules, such as *racemic* 1,1'-ethylenedi-η^5-indenylzirconium dichloride.[17] Whereas polymer configuration in heterogenous catalysis depends on the chirality of the crystal lattice, the chirality of the molecule of the transition metal compound dictates configuration in homogeneous catalysis.

The effects of steric and electronic modification of Cp rings on olefin polymerization has been reviewed.[18] The wide range of polymerization conditions and a lack of quantitative evaluations has hampered drawing definitive conclusions. However, some general themes are apparent. In $(CpR)_2MCl_2$ catalysts, electronic effect of R on polymerization activity dominate over steric effects. The electron withdrawing groups enhance catalytic activity, presumably by increasing electrophilicity of the metal, resulting in more facile olefin coordination and insertion. Steric effects play a minor role in polymerization activity unless R or the olefin are rather large and the metal is small (Ti

vs. Zr). Steric considerations are thought to be more important in controlling the tacticity of the polymer.

Olefin Polymerization Catalysts Supported by Nitrogen Containing Ligands

Modification of Cp ligands is not trivial. For that reason, as well as the plethora of patents on Cp systems, investigation into non-Cp Ziegler-Natta catalysts has intensified. In the following section, some examples of ligands systems currently under consideration are discussed. All of the systems mentioned have the advantage of easily adjustable electronic and steric properties. It should also be noted that in cases where polymerization is observed, activities are usually far lower than that of metallocenes.

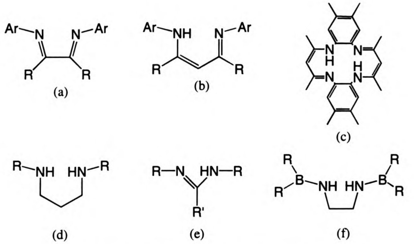

Figure 6 Examples of Cp Alternatives

α-diimines

There are late transition metal catalysts supported by α-diimines ligands (Figure 6(a) $L^{(a)}$), which are active for olefin polymerization.[19-21] In the most significant instances, Brookhart has successfully polymerized ethylene and other α-olefins to high molecular

weights (at 1-4 atm and 0-25 °C) with $[(ArN{=}C(R)C(R){=}NAr)M(CH_3)(OEt_2)]$ $[B(3,5\text{-}C_6H_3(CF_3)_2)_4]$ (M=Pd or Ni, Ar = 2,6-diisopropyl benzene, R = Me or H).[20] Using a similar system, the first copolymerization of ethylene and propylene with polar-functionalized vinyl monomers to high molecular weight was also reported.[21] These results are improvements over most late metal Ziegler-Natta type catalysts which tend to dimerize or oligomerize olefins due to β-hydride elimination.[22] Brookhart found that reducing the steric bulk of the ligand by replacing the 2,6-diisopropyl benzene with 2,6-dimethylbenzene resulted in less branched, more linear polymer with a decreased molecular weight. The mechanism proposed in Figure 7 was based on exhaustive NMR studies. The rate of exchange of bound ethylene on $L^{(a)}Pd(Me)(OEt_2)$ with free ethylene is dependent on ethylene concentration. Ethylene displacement of the α-olefin in formation of D in Figure 7 was therefore assumed to be a dissociative mechanism requiring coordination of the ethylene to an axial position on the metal. The ortho substituents on the aryl groups are arranged as to interfere sterically with such an approach. As a result, when the ortho substituents are large, the chain termination transition state is disfavored and longer polymer chains (ie., higher molecular mass polymers) are produced. Brookhart's system nicely demonstrates the importance that even small changes of ligand steric properties can have on catalyst reactivity.

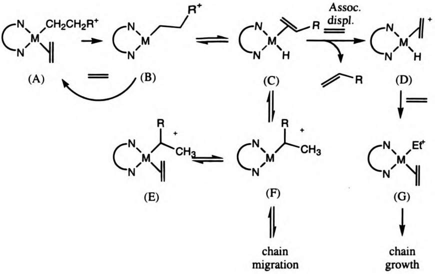

Figure 7 Brookhart Polymerization Mechanism

β-diketimine

Similar to α-diimines, β-diketimine (or bis(ketenimine)) (Figure 6(b) $L^{(b)}$) ligands are prepared by reaction of β-diketones with primary amines.[23] Most usage of β-diketimines has been with late transition metals.[19,23,24] There are examples of β-diketimine main group compounds.[25,26] Surprisingly, little work has been carried out with early transition metals.[27-29] Lappert synthesized $L^{(b)}*MCl_3$ ($L^{(b)}*$ = $^tBuC(NR)CHC(NR)Ph$, R = $SiMe_3$, M = Zr, Hf)(**1**) in 1994.[27] It is interesting to note that the ligand synthesis for this compound is not the usual condensation of primary amines and a β-diketone. Lappert found that reaction of $LiCH(SiMe_3)_2$ with ^tBuCN results in the formation of $[C(SiMe3)HC(^tBu)CN(SiMe_3)Li]_2$ (Figure 8). Adding two equivalents of PhCN to this complex results in the formation of $[L^{(b)}*Li]_2$ which was then reacted with $ZrCl_4$ to give $L^{(b)*}ZrCl_3$.

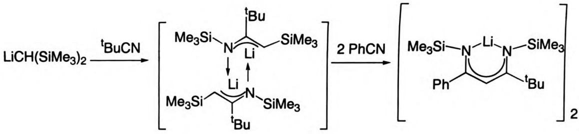

Figure 8 Lappert Ligand Preparation

It was only recently that Collins prepared several β-diketimine compounds of the type $L^{(b)}ZrX_3$ and $(L^{(b)})_2ZrX_2$ (Ar = phenyl, R = methyl in Figure 6(b)).[28] Alkane elimination reactions were used to prepare $L^{(b)}Zr(CH_2Ph)_3$ from $Zr(CH_2Ph)_4$ and $L^{(b)}H$. Amine elimination reactions involving addition of one or two equivalents of $L^{(b)}H$ to $Zr(NMe_2)_4$ were used to synthesize $L^{(b)}Zr(NMe_2)_3$ and $(L^{(b)})_2Zr(NMe_2)_2$ respectively. $L^{(b)'}Zr(NMe_2)_3$ (Ar = *p*-$CF_3C_6H_4$ in Figure 6(b)) was prepared by the same methods. $(L^{(b)'})_2Zr(NMe_2)_2$ was not thermally stable and could not be isolated in pure form. Chloro derivatives ($L^{(b)}ZrCl_3$, $L^{(b)'}ZrCl_3$, and $(L^{(b)})_2ZrCl_2$) were prepared by reaction of the dimethylamido compounds with $Me_2NH(HCl)$ or Me_3SiCl.

Collins was able to alkylate the chloro derivatives with MeLi or $PhCH_2MgCl$ to give $(L^{(b)})_2Zr(CH_2Ph)_2$ and $(L^{(b)})_2ZrMe_2$. Reaction of the chloro derivatives with CpLi and IndLi also gave $L^{(b)}ZrCpCl_2$, $L^{(b)}ZrIndCl_2$, and $L^{(b)'}ZrCpCl_2$.

After comparing X-ray structures of $(L^{(b)})_2Zr(NMe_2)_2$ and $L^{(b)}ZrIndCl_2$, Collins suggested that the β-diketimine ligands can modify their mode of coordination to the metal in response to the donor properties of the ancillary ligands. For example, in $(L^{(b)})_2Zr(NMe_2)_2$ with its strong π-donor ligands, the β-diketimine ligand presumably acts as a 2σ, $4e^-$ donor to give a 16 e^- compound. On the other hand, in the more electron

deficient L$^{(b)}$ZrIndCl$_2$, hapticity of the β-diketimine ligand shifts from η^2 to η^5 to increase π coordination of the ligand to the metal . The π-donation from the β-diketimine ligand, however, is assumed to be weak.

Octamethyltetraazaannulene (Me$_8$taa)

Me$_8$taa (Figure 6(c)), a macrocyclic analog of β-diketimines, has been used by Jordan[30] to stabilize group 4 transition metals. This ligand is prepared via a Ni-templated condensation of 2,4-pentanedione and 4,5-dimethyl-1,2-phenylenediamine. Salt-elimination, alkane-elimination, and amine-elimination reactions similar to those described previously were used to synthesize chloride, alkyl, and amide complexes of the form (Me$_8$taa)MX$_2$ (X = Cl, Me, CH$_2$SiMe$_3$, CH$_2$Ph, CH$_2$CMe$_3$, NMe$_2$, NEt$_2$ M = Zr, Hf). All of the resulting complexes have a *cis* out of plane structure (Figure 9).

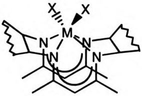

Figure 9 *cis*-Out of Plane Structure

Migration of a Zr bound methyl group to an electrophilic Me$_8$taa imine carbon was observed for (Me$_8$taa)ZrMe$_2$. This migration is accelereated by a Lewis base to yield (Me$_9$.taa)MX(base). Alkyl migrations did not occur in the bulkier zirconium analog (R = CH$_2$SiMe$_3$) or in the analogous halfnium compounds (R = Me, CH$_2$SiMe$_3$). Such migrations have been observed for the similar (Me$_4$taa)MR$_2$ and (Me$_4$taen)MR$_2$ complexes.[31]

The cationic species [(Me$_8$taa)MR$^+$][B(C$_6$F$_5$)$_4^-$], formed by protonolysis of (Me$_8$taa)MR$_2$ with [HNMePh$_2$][B(C$_6$F$_5$)$_4$] or [HNMe$_2$Ph][B(C$_6$F$_5$)$_4$] polymerized ethylene poorly. Jordan proposed that the [(Me$_8$taa)MR$^+$][B(C$_6$F$_5$)$_4^-$] compounds have a low tendency toward formation of π complexes with alkenes and alkynes.

Diamines

The first example of living polymerization of aliphatic α-olefins at room temperature was reported by McConville.[32] The cationic alkyl complex derived by methyl anion abstraction from the diamine compound [ArN(CH$_2$)$_3$NAr]TiMe$_2$ (Ar = 2,6-diisopropylbenzene, 2,6-dimethylbenzene) is the catalyst that performs this living polymerization. The diamine ligands in this report (Figure 6(d), L$^{(d)}$) were prepared by reaction of two equivalents of LiNHAr with Br(CH$_2$)$_3$Br (two equivalents of tetramethylethylenediamine were necessary to prevent formation of an undesired elimination product, ArNHCH$_2$CH=CH$_2$).

McConville also reported the polymerization of aliphatic α-olefins by [ArN(CH$_2$)$_3$NAr]TiX$_2$ (X = Cl, Me Ar = 2,6-diisopropylbenzene, 2,6-dimethylbenzene) activated with methylaluminoxane (MAO).[33] Zirconium analogs of the type L$^{(d)}$ZrX$_2$ (X = Cl, NMe$_2$, Me, CH$_2$Ph) have also been synthesized.[34] Polymerization (as well as production of oligomers) of 1-hexene was observed when L$^{(d)}$ZrMe$_2$ was activated with MAO at 68 °C. Chain end analysis suggests that a cationic alkyl [L$^{(d)}$ZrP]$^+$ (P = polymer) inserts 1-hexene in a 1,2 fashion (similar to the L$^{(d)}$TiMe$_2$ system) followed by β-hydride elimination. It appears that chain transfer to the aluminum (and not β-hydride elimination) is the mechanism of chain termination in the titanium/MAO system, as

olefinic resonances have not been observed *in the* $^{13}C\{^{1}H\}$-*NMR* spectra of the polymer or oligomers produced.

As opposed to $L^{(d)}TiMe_2/B(C_6F_5)_3$, which produced a living polymerization at 23 °C, $L^{(d)}ZrMe_2/B(C_6F_5)_3$ was not active for polymerization 1-hexene at 23 °C. Reaction of equimolar amounts of $L^{(d)}ZrMe_2$ and $\{Ph_3C\}[B(C_6F_5)_4]$ did oligomerize 1-hexene at 23 °C, but no evidence of high polymer was found.

Amidinates

Amidinate ligands (Figure 6(e) $L^{(e)}$) are used frequently to prepare various types of complexes with main group,[35] transition[36,38] and lanthanide[37] metals. These bidentate ligands are four electron donors with a small chelating angle (~115°). The steric properties are thought to lie somewhere between those of Cp and Cp*.[37] Being "harder" in character than Cp, amidinates should form highly polarized M-N bonds leading to a more electrophilic metal.[37,41]

Eisen has reported that generation of 'cationic' compounds from reaction of $(L^{(e)})_2ZrCl_2$ (R = $SiMe_3$ and R' = Ph or tolyl) with MAO resulted in polymer active catalyst.[38] It was observed that smaller ratios of MAO/catalyst improved the catalytic activity and molecular weights of the polymer. The opposite is true of early transition metal Cp systems[39] where the high amounts of MAO cocatalyst required can limit economic viability. These increases are attributed to the role of MAO in chain termination processes (alkyl transfer, etc.,).

Rausch has synthesized the titanium amidinate compounds $L^{(e)}Ti(O^{i}Pr)_3$, $\{L^{(e)}TiCl_3\}_2$, $L^{(e)}TiCl_3(THF)$, and $L^{(e)}TiCl_3(PMe_3)$ (R = $SiMe_3$ and R' = Ph) and found

them to be active in the polymerization of styrene when activated with MAO.[40] The resulting polymer was highly syndiotactic. $\{L^{(e)}TiCl_3\}_2$ had the highest activity followed by $L^{(e)}Ti(O^iPr)_3$. $L^{(e)}TiCl_3(THF)$, and $L^{(e)}TiCl_3(PMe_3)$ had the lowest activities due to the electron-donating THF and PMe_3 groups which greatly deactivate the metal. $(L^{(e)})_2TiCl_2$ did not polymerize ethylene.

$\{L^{(e)}TiCl_3\}_2$, $L^{(e)}Ti(O^iPr)_3$, $(L^{(e)})_2TiCl_2$ and $(L^{(e)})_2ZrCl_2$ when activated with MAO were found to react very slowly with ethylene at 20 °C and not at all with polyethylene under similar conditions.

Surprisingly, $(L^{(e)})_2ZrMe_2$ and $(L^{(e)})_2TiMe_2$ were found to be inactive for polymerization of ethylene or propylene when activated with $Ph_3C[B(C_6F_5)_4]$. However, Arnold has isolated $(L^{(e)})_2ZrMe[MeB(C_6F_5)_3]$ from reaction of $(L^{(e)})_2ZrMe_2$ with $B(C_6F_5)_3$. This species was found to be moderately active toward ethylene polymerization.[41]

Richeson was able to prepare an amidinate family consisting of $(L^{(e)})_2MCl_2$ (R = cyclohexane, R' = Me for M = Zr, Ti, Hf and *tert*-butyl for M = Zr) and $(L^{(e)})_2MMe_2$ (R' = Me, M = Zr).[42] All compounds polymerize ethylene when activated with MAO. Lowering the ratio of MAO/catalyst resulted in slight increase in molecular weight similar to Eisen's findings.

bis(borylamines)

Schrock has synthesized group 4 transition metal complexes stabilized by the bis(borylamine) ligand $[Mes_2BNCH_2CH_2NBMes_2]^{2-}$ (Ben^{2-}) (Figure 6(f)).[43] The Ben ligand is made by reaction of $H_2NCH_2CH_2NH_2$ with (1) 2LiBu/THF and (2) $2Mesityl_2BF$

to yield $Mes_2BNHCH_2CH_2NHBMes_2$ (H_2(Ben)). Schrock was able to synthesize the dichlorides (Ben)$TiCl_2$ and (Ben)$ZrCl_2$(THF). From the former, monoalkyl- and dialkyltitanium derivatives were made ((Ben)TiRCl (R = CH_2Ph, CH_2CMe_3) and (Ben)TiR_2 (R = CH_2Ph, Me) by reaction with corresponding Grignard reagents. Though (Ben)$ZrMe_2$ was prepared analogously, it was less thermally stable than (Ben)TiR_2 and was found to undergo metallation of an ortho methyl group to form a dicyclometalated compound. Reaction of (Ben)$TiMe_2$ with $B(C_6F_5)_3$ results in [(Ben)TiMe][$MeB(C_6F_5)_3$] which did not polymerized ethylene readily at 25 °C and 1-2 atm possibly in part due to a strong binding of the anion to the metal. Schrock concludes that a steric increase on the Ben ligand is required to expel the $[MeB(C_6F_5)_3]^-$ in the presence of ethylene and also to prevent the dimerization observed in (Ben)$ZrMe_2$.

Application of β-diketimines to Asymmetric Synthesis

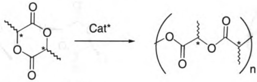

Figure 10 Polylactides

Polylactide materials (Figure 10) are ideal for employment in a wide range of medicinal applications from absorbable wound dressings and sutures to controlled release drug capsules, because they are biocompatible, biorenewable, and biodegradable. As with any polymer, controlling the properties of the polymer to best fit the desired application is paramount.

Tin and zinc octanoates, $M(O_2CR)_2$, are the most common dilactide polymerization catalysts.[44] Catalysts of this type offer little in the way of electronic or steric adjustability. Also, they have several sites of polymer initiation leading to multiple chain transfers and an ill-defined polymerization. A catalyst with tunable steric and electronic properties and a single initiation site would be more ideal.

The cyclic monomer 3,6-di(alkyl or aryl)-1,4-dioxane-2,5-dione (dilactone) contains two chiral centers and can form a polylactide by a ring-opening polymerization (ROP). By adjusting the electronic and steric environment of the catalyst, one might achieve kinetic resolution via polymerization of a racemic modification of dilactone. Potentially, catalytically selective polymerization of one enantiomer (and the meso-monomer (ex. R, R and R,S)) would leave the S,S monomer in solution (Figure 11). The S,S monomer could then be polymerized into a stereoregular polymer (S,S) or hydrolyzed to produce the enantiomerically pure lactic acid derivatives.

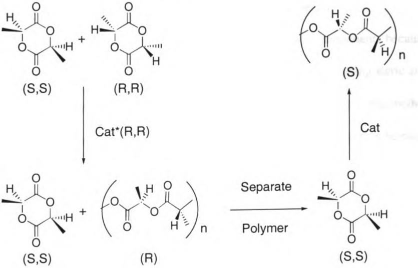

Figure 11 Kinetic Resolution of Polylactides Via Polymerization

In order to encourage and sustain polymerization, a highly electrophilic metal is desired in an asymmetric catalyst. The ligand sphere is designed to control the reactivity of that metal. It should ultimately be composed of two parts: an active moiety and an inert moiety. The active moiety is responsible for initiating the reaction and should be easily dissociated from the metal. The inert moiety should be unreactive and control the activity and stereoselectivity of the reaction. This inert moiety must have adjustable steric and electronic properties, so it can be customized to exclusively select (or exclude) a particular substrate.

We are interested in exploring the polymerization activity of compounds with group 4 transition metals. Plus four (d^0) oxidation states yield a highly electrophilic metal. As a consequence, they tend to form bonds that are more ionic in character. This increased polarization causes these bonds to be innately more reactive (a beneficial quality for ligands that might initiate polymerization (ie. active moiety)).

Bis mono- and diketimines ligands are employed as the inert components because their facile synthesis from 2,4-pentadione and primary amines facilitates tuning steric and electronic properties by varying the amine. The alkene proton (at ~ 6 – 4 ppm) and methyl protons (at ~ 2 ppm) also provide diagnostic ^{1}H NMR spectroscopic handles. A schematic of the general synthesis is shown in Figure 12.

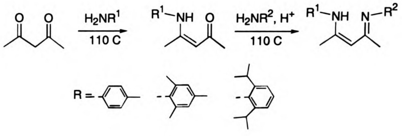

Figure 12 General Ligand Synthesis

Initial stages of this project involve synthesizing a family of compounds of the type L_2MX_2 (Figure 13) and surveying their reactivity. Then, using different groups for R^1 and R^2, chiral transition metal complexes may be synthesized. These chiral complexes could ultimately be used as asymmetric polymerization catalysts.

As racemic mixtures of these compounds may be difficult to separate, utilization of amino acids (L-phenylalanine, L-cysteine, L-valine, etc) and other chiral R groups are of interest. Figure 13 demonstrates how a chiral metal produces a pair of enantiomers, which may be difficult to resolve. On the other hand, a chiral metal with a chiral ligand (R = L-phenylalanine) produces diastereomers, which should be resolvable by fractional crystallization.

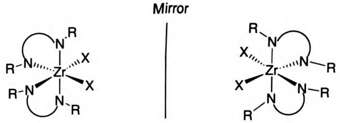

a) Enantiomers

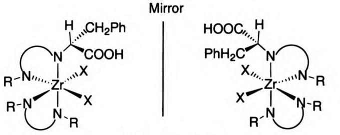

b) Diastereomers

Figure 13 Synthesizing Diastereomers vs. Enantiomers

What follows are details of the syntheses and characterizations of a family of compounds that show promise as precursors to asymmetric catalysts.

Chapter 2

RESULTS AND DISCUSSION

Ligand Synthesis

Synthesis of diketimine **2b** (Figure 14) was of interest because of the large sterically demanding R groups. Figure 14 summarizes the results of this effort (see Chapter 3 for experimental details).

The syntheses proceeded well with the exception of the final step (the second amine condensation). The large bulk of the R group probably inhibits condensation of the second amine. Successful synthesis of other sterically demanding ligand systems (namely $R^1 = R^2 =$ mesityl or 2,6-diisopropylphenyl) suggest that this step may indeed be achievable in good yields. Compound **2a** (4-(bis 3,5-(3,5-di-tert-butylphenyl)-phenylimino)-pent-4-en-2-one) is potentially useful as the monoimine or in combination with a second less bulky amine (ie., *p*-tolyamine or alkylamines). The large R group might be effective as a blocking group. At the very least, the preparation of compound **2a** demonstrates some of the versatility in amine synthesis that may be applied to ligand design.

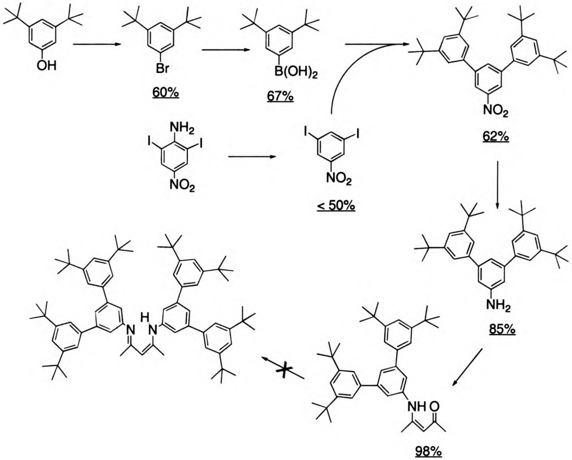

Figure 14 Scheme for Synthesis of 2b

Synthesis of LMX_3 and L_2MX_2 Type Compounds via Lithium Salt Metathesis

Previously in our group, a family of monoketimines consisting of $(TP)_2ZrCl_2$, $(TP)_2TiCl_2$ and $(TMP)_2TiCl_2$ (TP = 4-p-tolylimino-pent-4-en-2-one and TMP = 4-(2,4,6-trimethylphenylimino)-pent-4-en-2-one) were synthesized via metathetic reactions and fully characterized.[45] The general synthesis of L_nMCl_x compounds was achieved via a lithium salt metathesis method. The general scheme is shown in Eq (1) (Li(L) = Li(TTP) and Li(DDP), M = Ti or Zr).

$$\text{Eq (1)} \quad MCl_4 + nLi(L) \rightarrow (L)_nMCl_{4-n} + nLiCl$$

The lithium salts of the β-diketimine ligands were prepared in excellent yield by reaction of the β-diketimine free base with *n*-butyl lithium. The ligand lithium salt was collected from ether as light colored precipitate (white to yellow).

Addition of two equivalents of the lithium salt of the TTPH ligand (Li(TTP)) to a stirred toluene suspension of $ZrCl_4(THF)_2$ resulted in the formation of $(TTP)_2ZrCl_2$ (**3**) in 50% yield. The significant shift of the backbone alkene proton resonance from 4.67 ppm for Li(TTP) to 5.34 ppm was indicative of metal coordination. The room temperature ^1H NMR spectrum exhibits two methyl resonances, one corresponding to the tolyl moieties and the other corresponding to the ligand backbone (Table 1). Upon cooling (-50 °C), four methyl signals are observed suggesting *cis*-chloride configuration and a C_2 symmetry. An X-ray crystal structure (Figure 16 and Appendices that contain X-ray collection parameters and bond lengths and angles) indicates a C_2 symmetry with *cis* arrangement of the chlorides in an octahedral metal environment. $(TTP)_2ZrCl_2$ obviously interchanges between enantiomers at room temperature. An analogous compound,

$(PPP)_2ZrCl_2$ (PPPH = 2-phenylamino-4-phenylimino-2-pentene), was prepared by Collins via reaction of $(PPP)_2Zr(NMe_2)_2$ and two equivalents of $[Me_2NH_2][Cl]$.[28] $(PPP)_2ZrCl_2$ demonstrates similar spectroscopic characteristics. The Bailar twist mechanism[46] (Figure 15) proposed for $(PPP)_2ZrCl_2$ also accounts for the observed fluxional behavior of $(TTP)_2ZrCl_2$. In both cases, the enantiomers interconvert rapidly on the NMR time scale via a trigonal prismatic intermediate in which both backbone methyls (and both tolyl methyls respectively in the case of **3** are equivalent).

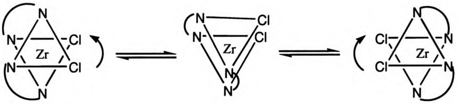

Figure 15 Bailar Twist Mechanism

Table 1 ^1H NMR Data for $(TTP)_2ZrCl_2$, $(TTP)TiCl_3$, and Li(TTP)

Compound	δ ppm	Appearance	Assignment
Li(TTP)	6.91	d, 4 H, *J* = 8.0 Hz	aromatic
($CDCl_3$)	4.01	d, 4 H, *J* = 8.0 Hz	aromatic
	4.35	s, 1 H	alkene
	2.25	s, 3 H	$CH_{3\ \mathrm{tolyl}}$
	1.61	s, 3 H	$CH_{3\ \mathrm{backbone}}$
$(TTP)_2ZrCl_2$	7.01	d, 4 H *J* = 8.1 Hz	aromatic
($CDCl_3$)	6.71	br s, 4 H	aromatic
	5.34	s, 1 H	alkene
	2.28	s, 6 H	$CH_{3\ \mathrm{tolyl}}$
	1.63	s, 6 H	$CH_{3\ \mathrm{backbone}}$
$(TTP)TiCl_3$	7.23-.13	m, 8 H	aromatic
($CDCl_3$)	6.03	s, 1 H	alkene
	2.36	s, 6 H	$CH_{3\ \mathrm{tolyl}}$
	2.12	s, 6 H	$CH_{3\ \mathrm{backbone}}$

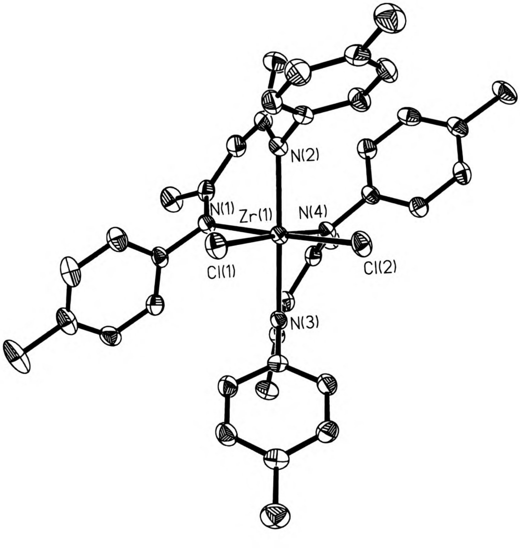

Figure 16 ORTEP Diagram of (TTP)$_2$ZrCl$_2$

$(TTP)_2ZrCl_2$ was found to initiate the polymerization of 3,6-dimethyl-1,4-dioxane-2,5-dione (dilactone) when combined with 4-*tert*-butylbenzyl alcohol at ~180 °C.[47] Polymerization was identified by the appearance of a broad signals at ~5ppm and 1.53 ppm in ^1H NMR.

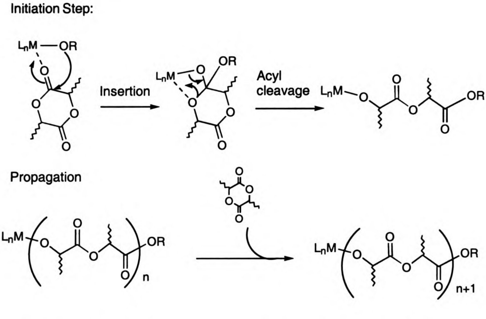

Figure 17 Cationic Mechanism of Ring Opening Polymerization

Figure 17 shows the probable mechanism for the polymerization.[44] Assuming this mechanism, an alkoxide group would replace a chloride forming HCl. The generation of HCl could destroy catalyst and is therefore undesirable. It also seems possible the alcohol may displace the ligand instead of the chloride. Loss of ligand results in loss of any possible reaction control. Complexes with alkoxides as initiating ligands are therefore better candidates. Efforts to prepare $L_nM(OR)_x$ type compounds have met with success (vide infra).

Reaction of one equivalent of Li(TTP) with $ZrCl_4(THF)_2$ gives only $(TTP)_2ZrCl_2$. However, Collins was able to make $(PPP)ZrCl_3$ by reaction of $(PPP)Zr(NMe_2)_3$ with three equivalents of Me_3SiCl.[28] $(TTP)ZrCl_3$ was synthesized analogously.[48]

Reaction of one equivalent of Li(TTP) with $TiCl_4$ gives $(TTP)TiCl_3$ (**4**) as dark purple crystals in 84% yield. The ^1H NMR spectrum shows a larger downfield shift of the backbone alkene proton (6.03 ppm) than in **3** (Table 1) An X-ray structure was obtained (Figure 18 and Appendices). The titanium appears to be five coordinate square pyramidal with chloride occupying the apical position and the other two chlorides and two nitrogens at the basal positions. The metal is out the plane of the ligand and seems to interact with the π-system of the diketimine in an "η^5" fashion evidenced by the puckering of the backbone. Lappert's compound **1** is similar to **4**. It also contains an out of plane metal, which may indicate η^5 character for the diketimine. The metal environment, in contrast to **4**, is described as distorted trigonal bipyramidal.[27]

Reaction of one equivalent of Li(DDP) with freshly sublimed $ZrCl_4$ gives $(DDP)ZrCl_3$ (**5**) as yellow crystals in 51 % yield. The isopropyl methyls appear as a pair of diastereotopic doublets in the ^1H NMR spectrum (Table 2). An X-ray crystal structure (Figure 19 and Appendices) was determined. It showed the arrangement around the zirconium to be square pyramidal. One of the chlorides resides at the apical position with the other chlorides and the nitrogens basal. Others in our group have found that reaction of $(DDP)ZrCl_3$ with three equivalents of MeLi gives $(DDP)ZrMe_3$ in moderate yield.[48,50] The X-ray structure of this compound shows the atoms around the metal to be arranged in a square pyramid with a methyl group at the apical position.

Table 2 ^{1}H NMR Data for (DDP)$ZrCl_3$, (DDP)$ZrCl_3$(THF), (DDP)$TiCl_3$, and Li(DDP)

Compound	δ ppm	Appearance	Assignment
Li(DDP)	7.16	m, 6 H	aromatic
(C_6D_6)	4.86	s, 1 H	alkene
	3.10	sept, 4 H, J = 6.9 Hz	$CH(CH_3)_2$
	1.79	s, 6 H	$CH_{3\ \mathrm{backbone}}$
	1.17	d, 12 H, J = 6.9 Hz	$CH_{3\ \mathrm{isopropyl}}$
	1.14	d, 12 H, J = 6.9 Hz	$CH_{3\ \mathrm{isopropyl}}$
(DDP)$ZrCl_3$	7.43-.20	m, 6 H	aromatic
($CDCl_3$)	5.90	s, 1 H	alkene
	3.05	sept, 4 H, J = 6.9 Hz	$CH(CH_3)_2$
	1.94	s, 6 H	$CH_{3\ \mathrm{backbone}}$
	1.37	d, 12 H J = 6.9 Hz	$CH_{3\ \mathrm{isopropyl}}$
	1.18	d, 12 H, J = 6.9 Hz	$CH_{3\ \mathrm{isopropyl}}$
(DDP)$ZrCl_3$(thf)	7.15	s, 6 H	aromatic
(C_6D_6)	5.43	s, 1 H	alkene
	3.90	m, 4 H	THF
	3.58	sept, 4 H, J = 6.8 Hz	$CH(CH_3)_2$
	1.65	s, 6 H	$CH_{3\ \mathrm{backbone}}$
	1.54	d, 12 H, J = 6.8 Hz	$CH_{3\ \mathrm{isopropyl}}$
	1.10	d, 12 H, J = 6.8 Hz	$CH_{3\ \mathrm{isopropyl}}$
	1.05	m, 4 H	THF
(DDP)$TiCl_3$	7.20	m, 6 H	aromatic
($CDCl_3$)	6.26	s, 1 H	alkene
	2.97	sept, 4 H, J = 6.6 Hz	$CH(CH_3)_2$
	2.00	s, 6 H	$CH_{3\ \mathrm{backbone}}$
	1.33	d, 12 H J = 6.6 Hz	$CH_{3\ \mathrm{isopropyl}}$
	1.11	d, 12 H, J = 6.6 Hz	$CH_{3\ \mathrm{isopropyl}}$

Reaction of one equivalent of Li(DDP) with $ZrCl_4(THF)_2$ gives $(DDP)ZrCl_3(THF)$ (**6**) as small yellow crystals in 49% yield. The ^1H NMR spectrum is very similar to $(DDP)ZrCl_3$ (Table 2). $(DDP)ZrCl_3(THF)$ was also formed by adding excess THF to $(DDP)ZrCl_3$.

Reaction of one equivalent of Li(DDP) with $TiCl_4(THF)_2$ was also attempted. The crude ^1H NMR spectrum exhibits a number of new resonances (Table 2). Especially promising is the signal at 6.62 ppm assigned to the alkene backbone proton. This large downfield shift from 4.87ppm (for Li(DDP), Table 2) suggests formation of a titanium chelated compound ($(TTP)TiCl_3$ alkene proton resonance is 6.03 ppm). A new septet is also apparent at 2.97 ppm as well as new isopropyl resonances (doublets at 1.33 ppm and 1.11 ppm). The initial ^1H NMR spectrum strongly suggests the formation of a new compound. Since $(DDP)_2ZrCl_2$ is not known to form (presumably due to steric restrictions imposed by the diisopropyl groups), it is assumed the smaller titanium derivative ($(DDP)_2TiCl_2$) would be even less likely to form. Therefore, the new product is proposed to be $(DDP)TiCl_3$ (**7**) Unfortunately, attempts to further purify this compound for ^{13}C-NMR, X-ray, and other analyses were unsuccessful.

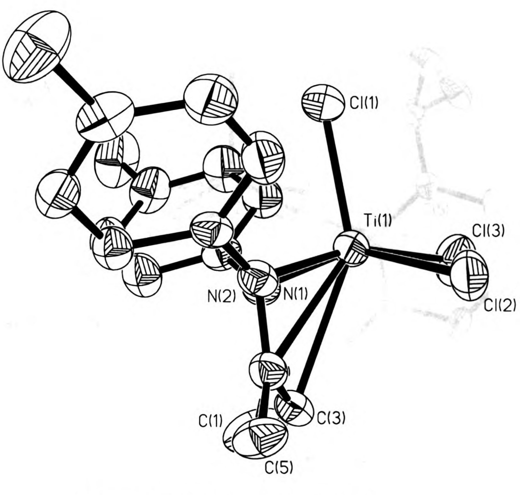

Figure 18 ORTEP Diagram of (TTP)TiCl$_3$

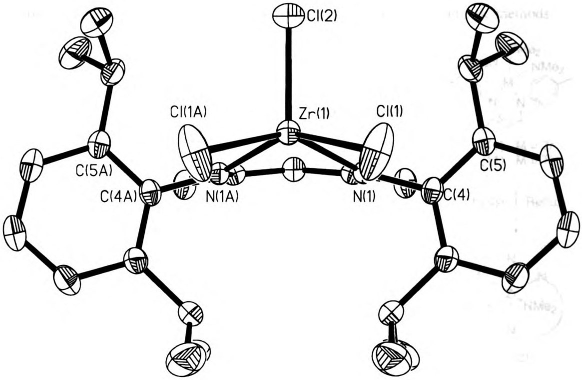

Figure 19 ORTEP Diagram of (DDP)ZrCl$_3$

Synthesis of LMX_3 and L_2MX_2 Type Compounds via Acid/Base Routes

Acid/base synthetic routes (Figure 20) were used to prepare LMX_3 (X = NMe_2 for M = Zr and Ti, X = CH_2Ph for M = Zr) and L_2MX_2 (X = NMe_2, M = Zr). The volatility of the reaction byproducts, the lack of Li salt residues, and the further acid/base reactivity of the remaining ancillary ligands make acid/base reactions attractive synthetic methods.

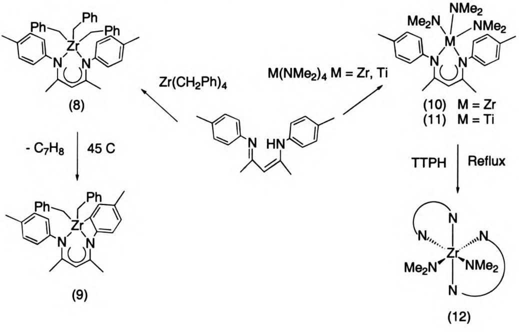

Figure 20 Acid / Base Routes

Reaction of one equivalent of TTPH with $Zr(CH_2Ph)_4$ at room temperature for 8 hours yielded yellow crystals of $(TTP)Zr(CH_2Ph)_3$ (**8**) from toluene in 78% yield. An X-ray structure of this compound was determined (Figure 22 and Appendices) which shows a five coordinate zirconium in a square pyramidal environment. One of the benzyl methylenes is at the apical position with the other two methylenes and two nitrogens (from the η^2-coordinated TTP) at the basal positions. The room temperature ^1H NMR

spectrum (Table 3) shows only one benzyl resonance at 2.61 ppm, rather than the two expected. This single resonance is maintained even at low temperatures. In contrast to the NMR data, the X-ray structure shows one benzyl should not be equivalent to the other two. The exchange of these benzyl groups must, therefore, be fast on the NMR time scale.

A second equivalent of TTPH was added to (TTP)Zr(CH_2Ph)$_3$ in an attempt to prepare (TTP)$_2$Zr(CH_2Ph)$_2$. After heating at 45 °C for several hours, the ^{1}H NMR spectrum showed many new peaks, but no change in the TTPH signals. A NMR tube sample of (TTP)Zr(CH_2Ph)$_3$ alone was then heated for 48 hours at 45 °C in C_6D_6. The resulting ^{1}H NMR spectrum was clean and contained many new resonances with complete loss of signals from starting material ((TTP)Zr(CH_2Ph)$_3$). From the NMR data, it was apparent that toluene was formed. Also, two separate backbone methyl resonances and two separate tolyl methyl resonances were observed suggesting a lower symmetry structure. After integrating the ^{1}H NMR spectrum, it was determined that only one equivalent of toluene was lost. Based on the low symmetry and a downfield resonance at 7.80 ppm (1 H, assumed to be due to a lone carbene proton), the first structural proposal was that a carbene had been formed through α-hydrogen abstraction (Figure 21). If this were the case, a pair of diastereotopic hydrogens would be expected for the remaining benzyl methylene. Doublets at 2.13 and 1.66 ppm (J = 9.6 Hz) were assigned to be due to such protons. Unfortunately, these signals corresponded to four hydrogens instead of two expected for a carbene structure, so the proposed structure was incorrect.

A second formulation, (η^3–MeC(NC_7H_6)CHC(N–*p*–Tol)Me)Zr(η^2–CH_2Ph)(η^1–CH_2Ph) ((TTP*)Zr(CH_2Ph)$_2$ (**9**)), resulting from an ortho-metallation of one of the tolyl groups was proposed (Figure 21). This structure accounts perfectly for the NMR data

(Table 3). An X-ray structure was determined for this compound, which supports the proposed ortho-metallated structure (Figure 23 and Appendices). The tolyl group coordinates to the zirconium at the carbon ortho to the nitrogen. The X-ray structure also shows one benzyl group is η^2, exhibiting a Zr-C_{ipso} interaction (Zr(1)-C(28) = 2.58 Å) and an acute C(21)-C(20)-Zr(1) angle of 83.58°. The structure of $Zr(CH_2Ph)_4$ has 85° as its most acute C-C-Zr angle.[49] The other benzyl group in **9** appears to be η^1, which leads to different environments for the two sets of methylene protons. This difference is not apparent in the room temperature or low temperature ^1H NMR spectra suggesting that the exchange of the benzyl groups is rapid on the NMR time scale.

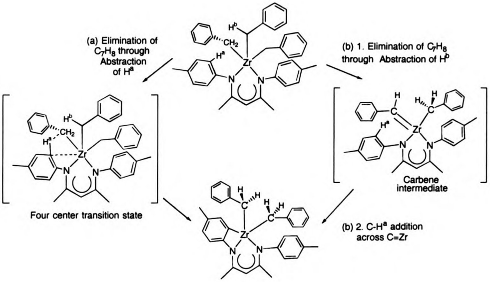

Figure 21 Possible Thermolysis Mechanisms of (TTP*)$Zr(CH_2Ph)_2$

Table 3 ^{1}H NMR Data for (TTP)Zr(CH_2Ph)$_3$, (TTP*)Zr(CH_2Ph)$_2$, and TTPH

Compound	δ ppm	Appearance	Assignment
TTPH	6.91	d, 4 H, J = 8.6 Hz	aromatic
(C_6D_6)	6.84	d, 4 H, J = 8.6 Hz	aromatic
	4.81	s, 1 H	alkene
	2.10	s, 3 H	$CH_{3\,\mathrm{tolyl}}$
	1.84	s, 3 H	$CH_{3\,\mathrm{backbone}}$
(TTP)Zr(CH_2Ph)$_3$	7.10	m, 6 H	aromatic
(C_6D_6)	6.90	m, 7 H	aromatic
	6.73	m, 10 H	aromatic
	5.06	s, 1 H	alkene
	2.61	s, 6 H	$CH_{2\,\mathrm{benzyl}}$
	2.09	s, 6 H	$CH_{3\,\mathrm{tolyl}}$
	1.62		$CH_{3\,\mathrm{backbone}}$
(TTP*)Zr(CH_2Ph)$_2$	7.80	m, 1 H	aromatic
(C_6D_6)	7.18-6.75	m, 13 H	aromatic
	6.48	d, 4 H	aromatic
	5.31	s, 1 H	alkene
	2.33	s, 3 H	$CH_{3\,\mathrm{tolyl}}$
	2.13	d, 2 H, J = 9.6 Hz	$CH_{2\,\mathrm{benzyl}}$
	2.13	s, 3 H	$CH_{3\,\mathrm{tolyl}}$
	2.07	s, 3 H	$CH_{3\,\mathrm{backbone}}$
	1.66	d, 2 H, J = 9.6 Hz	$CH_{2\,\mathrm{benzyl}}$
	1.58	s, 3 H	$CH_{3\,\mathrm{backbone}}$

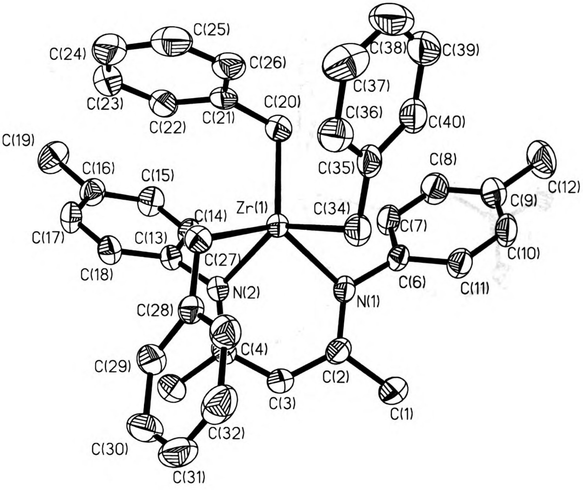

Figure 22 ORTEP Diagram of (TTP)Zr(CH$_2$Ph)$_3$

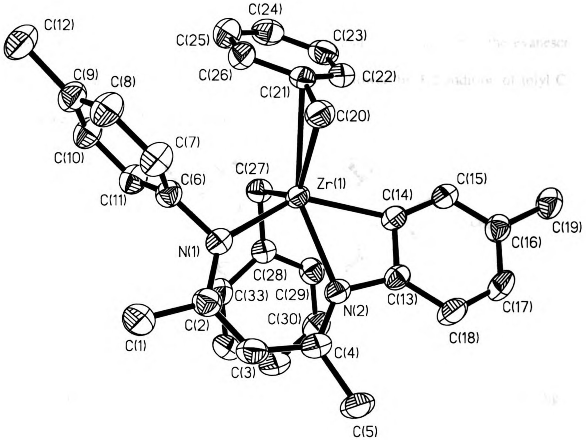

Figure 23 ORTEP Diagram of the Thermolysis Product

There are two possible mechanisms by which this thermolysis could occur. The toluene could be formed from a direct σ-bond metathesis of a tolyl proton (*H1*) via a four center transition state. This mechanism is illustrated in Figure 21(a). The abstracted proton may also come from an adjacent benzyl ligand (*H2*) resulting in the evanescent formation of a carbene. This formation would be followed by 1,2-addition of tolyl C-H across a Zr=C bond (Figure 21(b)).

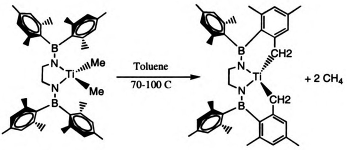

Figure 24 Thermolysis of BenTiMe$_2$ to (TwistBen)Ti

Similar alkyl elimination has been observed and studied in Schrock's Ben ligand system (Figure 6(f)).[43] BenTiMe$_2$ eliminates two equivalents of methane to yield an orthometallated product which Schrock refers to as TwistBen (Figure 24). Direct σ-bond metathesis and α-abstraction followed by 1,2-addition of an ortho methyl across the Ti=CH$_2$ bond were proposed as possible mechanisms. Schrock prepared the deuterated BenTi(CD$_3$)$_2$ and characterized the organic products of its thermolysis as only CD$_3$H. It was then concluded that the thermolysis of (Ben)TiMe$_2$ proceeds via a direct σ-bond metathesis. Products expected for α-abstraction-1,2-addition mechanism would be CD$_4$ and CD$_2$H$_2$.

To distinguish which mechanism might be at work in the case of (TTP)Zr(CH_2Ph)$_3$, deuterium-labeling studies were carried out in our group.[50] (PPP)Zr(CH_2Ph)$_3$ (PPP = 2-phenylamino-4-phenylimino-2-pentene) and the perdeutero (PPP-d^{10})Zr(CH_2Ph)$_3$ were prepared analogously to (PPP)Zr(CH_2Ph)$_3$. Thermolysis of (PPP)Zr(CH_2Ph)$_3$ afforded (PPP-)Zr(CH_2Ph)$_2$ and toluene by NMR at 65 °C. Likewise, (PPP-d^{10})Zr(CH_2Ph)$_3$ undergoes thermolysis at 65 °C to form (PPP-d^{10}-)Zr(CH_2Ph)$_2$ and $C_6H_5CH_2D$ by NMR. A characteristic triplet for $C_6H_5CH_2D$ was observed at 2.08 ppm (with J = 2 Hz). Formation of $C_6H_5CH_2D$ was also verified by GC-MS and independent synthesis. This experiment provides strong evidence for direct σ-bond metathesis (Figure 21(a)) as the mechanism for thermolysis of (TTP)Zr(CH_2Ph)$_3$.

No reaction of Zr(CH_2Ph)$_4$ with DDPH was observed, even after heating at 100 °C for ten hours. Presumably, the isopropyl groups impose a kinetic barrier against alkyl elimination.

Reacting Zr(NMe_2)$_4$ with TTPH at room temperature gave (TTP)Zr(NMe_2)$_3$ (**10**) as an orange-yellow solid in excellent yield (98%). The ^{1}H NMR spectrum (Table 4) suggests that the exchange of the NMe_2 is rapid on the NMR time scale as only one signal is observed instead of two. Collins has synthesized the phenyl substituted analog of this compound (PPP)Zr(NMe_2)$_3$.[28] The ^{1}H NMR data for these two compounds are very similar (chemical shift of (PPP)Zr(NMe_2)$_3$/(TTP)Zr(NMe_2)$_3$): backbone alkene proton (5.01/5.10 ppm), dimethylamine protons (2.73/2.80 ppm), backbone methyls (1.75/1.75 ppm). Suitable crystals for single crystal X-ray diffraction were grown from pentane and since no structure had been previously reported, a data set was collected and solved (Appendices). The ORTEP diagram in Figure 25 shows the nitrogens arranged around the

zirconium in a trigonal bipyramid orientation. Zr, N(2), N(3), and N(4) can be considered coplanar with the summation of the angles between them being 358.7°. Planarity observed in NMe_2 groups (average of Σ_{angles} 359.7°) is consistent with π-donation to the metal.

The titanium analogue of this compound was synthesized in the same manner from $Ti(NMe_2)_4$ and TTPH. Heating overnight at 35 °C was required to complete the reaction. Large orange crystals of $(TTP)Ti(NMe_2)_3$ (**11**) were obtained from pentane in 87% yield. The ^1H NMR data is comparable to $(TTP)Zr(NMe_2)_3$ (Table 4). An X-ray data set was solved for this compound in order to compare it to $(TTP)Zr(NMe_2)_3$ (Figure 26 and Appendices). The nitrogens of this compound also adopt a distorted trigonal bipyramidal arrangement around the titanium, and the NMe_2 groups are planar (Σ_{angles} 359.6°) as in compound **10**.

Table 4 ^1H NMR Data for $(TTP)Zr(NMe_2)_3$, $(TTP)Ti(NMe_2)_3$ and $(TTP)_2Zr(NMe_2)_2$

Compound	δ ppm	Appearance	Assignment
$(TTP)Zr(NMe_2)_3$	6.98	d, 4 H, *J* = 8 Hz	aromatic
(C_6D_6)	6.76	d, 4 H, *J* = 8 Hz	aromatic
	5.10	s, 1 H	alkene
	2.80	s, 18 H	$N(CH_3)_2$
	2.12	s, 6 H	$CH_{3\,\mathrm{tolyl}}$
	1.75	s, 6 H	$CH_{3\,\mathrm{backbone}}$
$(TTP)Ti(NMe_2)_3$	6.95	d, 4 H, *J* = 8 Hz	aromatic
(C_6D_6)	6.65	d, 4 H, *J* = 8 Hz	aromatic
	5.21	s, 1 H	alkene
	2.95	s, 18 H	$N(CH_3)_2$
	2.13	s, 6 H	$CH_{3\,\mathrm{tolyl}}$
	1.78	s, 6 H	$CH_{3\,\mathrm{backbone}}$
$(TTP)_2Zr(NMe_2)_2$	7.25	br s, 2 H	aromatic
(C_6D_6)	7.07	m, 2 H	aromatic
	6.87	m, 3 H	aromatic
	5.67	d, 1 H, *J* = 3 Hz	aromatic
	5.13	s, 1 H	alkene
	2.64	br s, 6 H	$N(CH_3)_2$
	2.22	s, 3 H	$CH_{3\,\mathrm{tolyl}}$
	2.06	s, 3 H	$CH_{3\,\mathrm{tolyl}}$
	1.77	s, 3 H	$CH_{3\,\mathrm{backbone}}$
	1.43	s, 3 H	$CH_{3\,\mathrm{backbone}}$

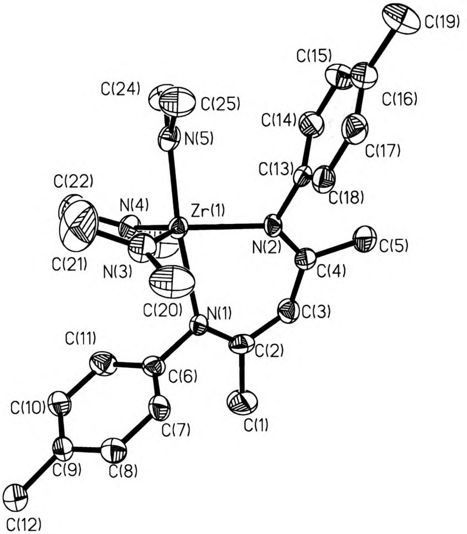

Figure 25 ORTEP Diagram of (TTP)Zr(NMe$_2$)$_3$

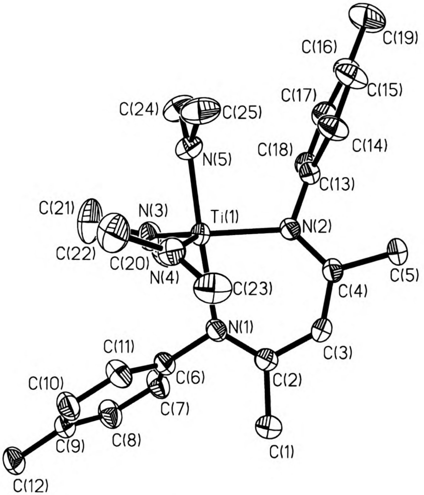

Figure 26 ORTEP Diagram of (TTP)Ti(NMe$_2$)$_3$

Adding a second equivalent of TTPH to (TTP)Zr(NMe_2)$_3$ (or reacting 2 : 1, TTPH : Zr(NMe_2)$_4$) results in the formation of (TTP)$_2$Zr(NMe_2)$_2$ (**12**) after heating at 90 °C for five hours. Recrystallization from pentane gave a 58% yield as orange-yellow crystals. Collins has also synthesized the phenyl analog ((PPP)$_2$Zr(NMe_2)$_2$) of this compound.[28] The ^{1}H NMR spectrum for (TTP)$_2$Zr(NMe_2)$_2$ (Table 4) is analogous to (PPP)$_2$Zr(NMe_2)$_2$. In both compounds two backbone methyl resonances are observed (and two tolyl methyl signals in **12**) indicating a *cis* arrangement of the dimethylamines in an octahedral geometry. Both compounds also display an unusually high field doublet (5.67 ppm for **12** and 5.8 ppm for (PPP)$_2$Zr(NMe_2)$_2$). This signal is due to an ortho hydrogen on an aromatic ring that is located directly over the shielding cone of an opposite aromatic ring. The proton experiences strong shielding causing it to resonate at higher field. No X-ray data were collected on **12**, as the structure of (PPP)$_2$Zr(NMe_2)$_2$ had already been reported. It adopts the anticipated distorted *cis* octahedral geometry and shows the 'upfield' ortho aromatic hydrogens pointing into the opposite rings. Due to the strong spectroscopic similarities, it is assumed that **12** exhibits the same structure as (PPP)$_2$Zr(NMe_2)$_2$. Attempts to prepare the titanium analog, (TTP)$_2$Ti(NMe_2)$_2$, from one equivalent of TTPH and (TTP)Ti(NMe_2)$_3$ or two equivalents of TTPH to one equivalent of Ti(NMe_2)$_4$ were unsuccessful even after refluxing overnight in toluene.

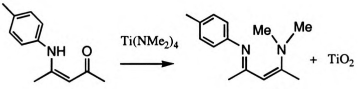

DTPH

Figure 27 Transamination to form DTPH

Previous work in our group has shown that reaction of TPH (TPH = 4-p-tolylimino-pent-4-en-2-one) with $Ti(NMe_2)_4$ results in a transamination to form 2-(dimethylamino)-4-(4-tolylimino)pent-2-ene (DTPH) (Figure 27).[45] Such transaminations have precedent.[51] After comparing ^1H and ^{13}C-NMR data, it was apparent that reaction of TPH with $Zr(NMe_2)_4$ does not result in transamination to form DTPH. Rather, $(TP)_2Zr(NMe_2)_2$ (**13**) is formed as yellow crystals in 66% yield. This difference was immediately evidenced by the difference in the shift of the diagnostic alkene hydrogen on the ligand backbone. The value is δ 4.76 ppm for DTPH compared to δ 6.66 ppm for $(TP)_2Zr(NMe_2)_2$ (Table 5). The melting point of $(TP)_2Zr(NMe_2)_2$ is also much higher at 164-6 °C than that of DTPH at 35-6 °C. Reaction of $(TP)_2Zr(NMe_2)_2$ with two equivalents of Me_3SiCl gave the previously characterized $(TP)_2ZrCl_2$[45] (by ^1H NMR (all signals match)).

Recalling that $(TTP)Zr(NMe_2)_3$ forms readily at room temperature and $(TTP)_2Zr(NMe_2)_2$ requires reflux in toluene, reaction of one equivalent of $Zr(NMe_2)_4$ and one equivalent of TPH gives $(TP)_2Zr(NMe_2)_2$ as the only product at room temperature. The difference in reactivity may be due to a more acidic proton in the monoketimine. The decrease in steric properties from the diketimine to the monoketimine ligand may also encourage the amine elimination.

The X-ray structure was solved for this compound (Figure 28 and Appendices) which confirmed the coordination of two equivalents of TP resulting in an octahedral arrangement around the metal. The oxygen atoms are arranged trans to each other. This trans arrangement is also observed in the X-ray structures of $(TP)_2ZrCl_2$ and $(TP)_2TiCl_2$.[45]

The dimethyl amido ligands are again more or less planar indicating considerable π donation.

Attempts to prepare (DDP)Zr(NMe_2)$_3$ from DDPH and Zr(NMe_2)$_4$ resulted in no reaction even after refuxing in toluene for ten hours. The ligand salt (DDP)H (HCl) was then added to a toluene solution of Zr(NMe_2)$_4$ at –77 °C. The reaction mixture was allowed to warm to room temperature over one hour. The toluene was removed and the solid was recrystallized from pentane to give small white crystals of (DDP)ZrCl(NMe_2)$_2$ (**14**) in 51% yield. The ^{1}H NMR resonances of this compound are very broad at room temperature, but sharpen at 50 °C (Table 5). An X-ray structure was obtained from one of the white crystals (Figure 29 and Appendices). There are two crystallographically unique molecules in the unit cell. The coordination around the Zr is distorted square pyramidal with one of the amine nitrogens in the apical position and the other three nitrogens and the chloride situated at the basal positions. The amino groups again indicate π donation with $\Sigma_{\text{angles}} = 359.8°$.

The reaction is probably facilitated by the protonolysis of one of the amido groups to give Zr(NMe_2)$_3$Cl. With the reduced sterics, a second aminolysis can proceed with loss of another equivalent of $HNMe_2$ to give (DDP)ZrCl(NMe_2).

This synthetic avenue may be useful if it proves to be general for various ligands and salt anions (Figure 33). Addition of a second equivalent of ligand followed by alcoholysis leads to single site species in which the X group can directly tune the metal electronics. Also, alkylating the chloride site with LiR, followed by alkyl abstraction could lead to single site cationic compounds. Coupling with other observed acid / base chemistry (vida infra) might lead to formation of a cationic imine compounds (Figure 33).

Table 5 ^{1}H NMR Data for $(TP)_2Zr(NMe_2)_2$, $(DDP)ZrCl(NMe_2)_2$ and $(TTP)Zr(NMe_2)(NC_6H_4CH_3)$

Compound	δ ppm	Appearance	Assignment
$(TP)_2Zr(NMe_2)_2$	6.97	s, 2 H	aromatic
(C_6D_6)	6.94	s, 1 H	aromatic
	6.66	s, 1 H	aromatic
	4.95	s, 1 H	alkene
	3.30	s, 6 H	$N(CH_3)_2$
	2.16	s, 3 H	$CH_{3\ \mathrm{tolyl}}$
	1.56	s, 3 H	$CH_{3\ \mathrm{backbone}}$
	1.42	s, 3 H	$CH_{3\ \mathrm{backbone}}$
$(DDP)ZrCl(NMe_2)_2$	7.12	s, 6 H	aromatic
(C_6D_6) at 50 °C	5.20	s, 1 H	aromatic
	3.03	sept, 4 H, $J = 6.9$ Hz	alkene
	2.70	s, 12 H	$N(CH_3)_2$
	1.63	s, 6 H	$CH_{3\ \mathrm{tolyl}}$
	1.37	d, 12 H, $J = 6.8$ Hz	$CH_{3\ \mathrm{backbone}}$
	1.15	d, 12 H, $J = 6.8$ Hz	
$(TTP)_2Zr(NMe_2)(p\text{-}NC_6H_4Me)$	6.91	d, 6 H, $J = 7.8$ Hz	aromatic
(C_6D_6)	6.74	d, 4 H, $J = 8.1$ Hz	aromatic
	6.36	d, 2 H, $J = 8.1$ Hz	aromatic
	5.30	s, 1 H	alkene
	2.78	s, 6 H	$NC_6H_4CH_3$
	2.26	s, 3 H	$N(CH_3)_2$
	2.11	s, 6 H	$CH_{3\ \mathrm{tolyl}}$
	1.82	s, 6 H	$CH_{3\ \mathrm{backbone}}$

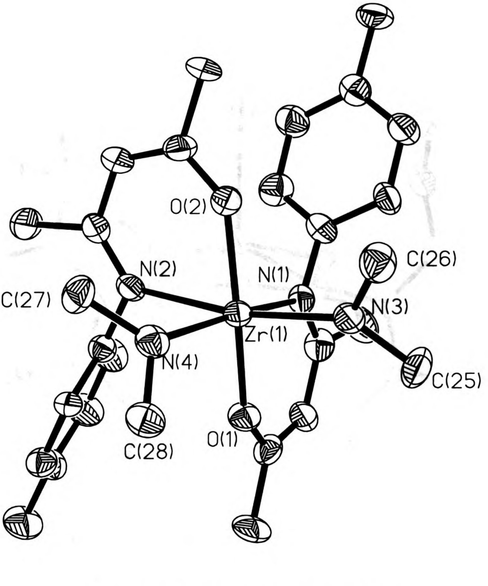

Figure 28 ORTEP Diagram of $(TP)_2Zr(NMe_2)_2$

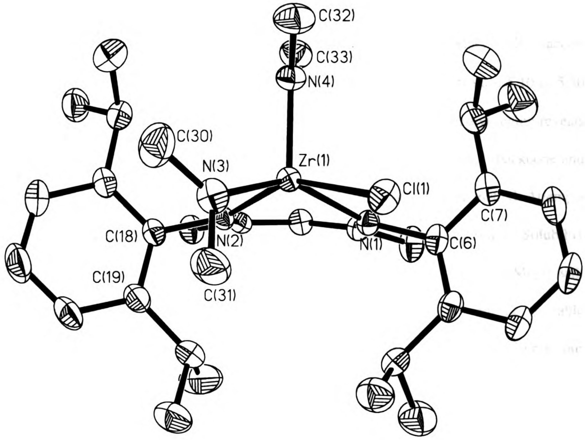

Figure 29 ORTEP Diagram of (DDP)ZrCl$(NMe_2)_2$

Further Acid/Base Chemistry

An attractive feature of compounds **10-15** is the possibility of replacing the NMe_2 groups through further acid/base chemistry. Initial exploration of this chemistry for compounds **10** and **12** has been successful. Assuming that the NMe_2 groups on (TTP)Zr(NMe_2)$_3$ are more basic than TTP, (TTP)Zr(NMe_2)$_3$ was reacted with one equivalent of *p*-toluidine at room temperature (Figure 30). Comparing the resulting ^1H NMR data (Table 5) to that of starting materials suggests that the product of the reaction is (TTP)Zr(NMe_2)(*p*-NC_6H_4Me) (**15**). The shift of the alkene proton from δ 5.10 to 5.30 ppm is the first indication of a reaction. Integrating the peaks in the methyl region reveals a 6 H:6 H:6 H:3 H ratio corresponding to two sets of 6 H from the ligand (backbone and tolyl methyls), 6 H from the dimethyl amine and 3 H from the toluidine methyl. Attempts to further purify the product through recrystallization were unsuccessful. Solubility problems hampered efforts to collect ^{13}C-NMR data. Reaction of (TTP)Zr(NMe_2)$_3$ with 2,4,6-trimethylaniline was also attempted. Some reaction occurred, but no tractable product was obtained. Further investigation into these 'imines' is warranted. These four coordinate zirconium compounds may exhibit interesting chemistry.

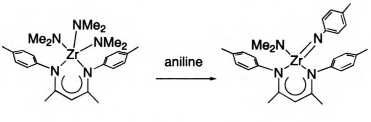

Figure 30 Aminolysis to Form an Imine

Other acid/base chemistry with the compounds of the type L$M(NMe_2)_3$ and $L_2M(NMe_2)_2$ has been observed in our group. Alcoholysis reactions (Figure 31) of these

compounds to yield the alkoxide derivatives have proven successful in some cases.[52] $(TTP)_2Zr(NMe_2)_2$ was reacted with two equivalents of methanol, *p*-cresol (4-methyl phenol) and 4-*tert*-butylbenzyl alcohol to give $(TTP)_2Zr(OMe)_2$, $(TTP)_2Zr(OC_6H_4Me)_2$ and $(TTP)_2Zr(OCH_2C_6H_4$-*t*-butyl$)_2$ respectively in good yields. Reaction of $(TTP)Zr(NMe_2)_3$ with three equivalents of methanol gave a low yield (< 5%) of $(TTP)Zr(OMe)_3$. Reaction of $(TTP)Zr(NMe_2)_3$ and $(TTP)Ti(NMe_2)_3$ with *p*-cresol and 4-*tert*-butylbenzyl alcohol resulted in intractable products.

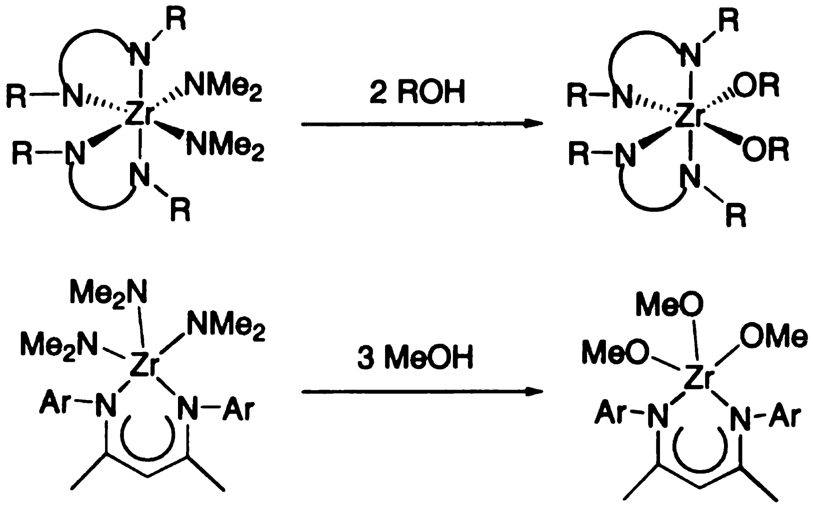

Figure 31 Alcoholysis of $LM(NMe_2)_3$ and $L_2M(NMe_2)_2$

Preliminary polymerization experiments with 3,6-dimethyl-1,4-dioxane-2,5-dione (dilactone) have been performed to survey the potential of these compounds.[52] All four compounds catalyze polymerization of dilactone as determined by the appearance of two broad signals in ^1H NMR spectra (5.13 and 1.53 ppm). Integration of monomer signals to polymer signals suggests that the order of activity is roughly (temperature of polymerization) $(TTP)_2Zr(OMe)_2$ (at 80-100 °C) < $(TTP)Zr(OMe)_3$ (at 80-100 °C) < $(TTP)_2Zr(OC_6H_4Me)_2$ (at 50-60 °C) < $(TTP)_2Zr(OCH_2C_6H_4$-*t*-butyl$)_2$ (at 40 °C). Though these results are preliminary, it is obvious from the temperature ranges alone, that the

alkoxides (catalyzing polymerization at 40 °C) are indeed better polymerization catalysts than the dichloride compound ((TTP)$_2$ZrCl$_2$, at ~180 °C). More detailed polymerization experiments are in progress.

CONCLUSIONS

Initial investigation of group 4 β-diketimines has shown their synthesis to be simple and versatile. The potential for preparing a much larger family of interesting compounds via acid/base and salt metathesis routes is clear (Figure 33). With this large library of derivatives available, the prospects for performing stereospecific polymerization remain bright. For example, the reaction below (Figure 32) suggests how a derivative of *trans*-1,2-diaminecyclohexane might react with (TTP)Zr(NMe$_2$)$_3$. The chirality of the *trans*-1,2-diaminecyclohexane derivative would be imposed on the complex. Once formed, the remaining dimethylamine might be replaced with an alkoxide through alcoholysis, leaving a single site chiral catalyst.

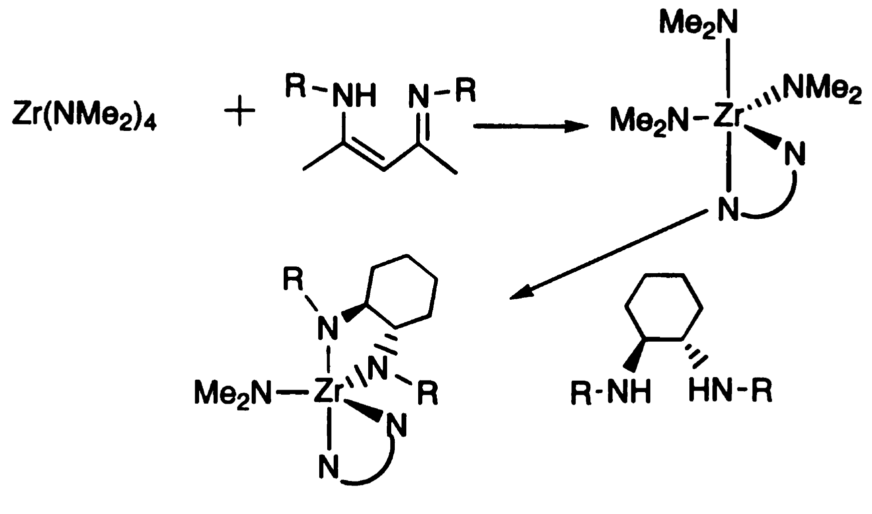

Figure 32 Proposed Aminolysis Reaction

Most Ziegler-Natta catalysts are presumed to initiate polymerization via a cationic species formed *in situ*. Alkyl abstraction reagents such as $[Ph_3C][B(C_6F_5)_4]$ and the strong Lewis base $B(C_6F_5)_3$ have been used to form such cationic species in metal alkyl and metal amine compounds. $[B(C_6F_5)_4]$ is generally too large to coordinate the metal as a ligand and instead results in generation of a cationic species. Our systems polymerize dilactones without activation. Accessing cations may improve catalytic activity. Figure 33 suggests some possible routes to cationic species.

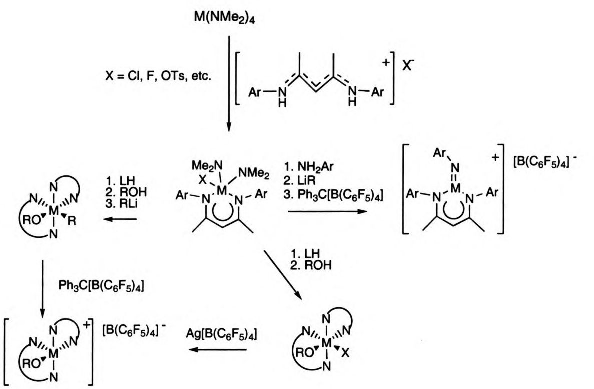

Figure 33 Other Possible Reactivity

CHAPTER 3

EXPERIMENTAL METHODS

Instrumental Procedures

^{1}H NMR spectra were recorded on Varian Gemini-300, Varian VXR-300, and INOVA-300 (299.949 MHz) spectrometers and referenced to residual proton solvent signals. ^{13}C spectra were recorded using Varian VXR-300 and INOVA-300 spectrometers operating at 75.430 MHz. Carbon chemical shifts are referenced to solvent signals. Low resolution mass spectra were obtained from powder samples on a portable Trio-1 VG Masslab Ltd. mass spectrometer. Analysis for carbon, hydrogen, and nitrogen were performed on a Perkin Elmer CHN 2400 Series II CHNS/O Analyser at the chemistry departement of Michigan State University or from Desert Analytics in Tucson, AZ.

Single Crystal X-Ray Structure Determination

Unless otherwise noted, all crystals were considered to be air sensitive and were collected by filtration and coated with Paratone–*N*. A suitable single crystal was selected and mounted onto a glass fiber (with Paratone-*N*). The crystal was then transferred to the goniometer of a Siemens SMART CCD diffractometer using Mo K_α radiation (λ = 0.71073 Å). Data were collected as 30 second per frame at 173 K. The initial cells were calculated by the Smart from three sets of 15 frames. All data sets were collected over a

hemisphere of reciprocal space. *SAINT* was used to integrate 1025 frames and to generate the *raw* file. Final unit cell parameters were obtained by least–squares refinement of strong reflections obtained. Absorption correction and time decay were applied to the data by *SADABS*. The non–hydrogen atoms located by using *SHELXS*–86 and refined using.

$(TTP)_2ZrCl_2$ (3). Large yellow crystals were grown from pentane/toluene at –30 °C. A data set was collected, solved, and refined in the space group $P2_1/n$ by direct methods.

$(TTP)TiCl_3$ (C_7H_8) (4). Small dark purple crystals were grown from pentane/toluene at –30 °C. A data set was collected, solved, and refined in the space group $P\bar{1}$ by direct methods.

$(DDP)ZrCl_3$ (5). Small almost colorless crystals were grown from pentane/toluene at –30 °C. A data set was collected, solved, and refined in the space group *Pnma* by direct methods.

$(TTP)Zr(CH_2Ph)_3$ (8). X-ray quality crystals were grown from toluene/pentane at –30 °C. A data set was collected, solved and refined in the space group *C2/c* by direct methods.

$(TTP^*)Zr(CH_2Ph)_2$ (9). Large orange round X-ray quality crystals were grown from pentane/toluene at –30 °C. A data set was collected, solved, and refined in the space group $P\bar{1}$ by direct methods.

$(TTP)Zr(NMe_2)_3$ (10). Large, yellow, X-ray quality crystals were grown from pentane/toluene at –30 °C. A data set was collected and partially solved in the space group *P*1. An inversion center between the two 'independent molecules' was observed. Its location was determined by calculating the difference of the absolute values of the x, y, and z coordinates for symmetrically related nitrogens. One of the two molecules was hemisphere of reciprocal space. SAINT was used to integrate 1025 frames and to generate the raw file. Final unit cell parameters were obtained by least-squares refinement of strong reflections obtained. Absorption correction and time decay were applied to the data by SADABS. The non-hydrogen atoms located by using SHELXS-86 and refined using.

$(TTP)_2ZrCl_2$ (3). Large yellow crystals were grown from pentane/toluene at −30 °C. A data set was collected, solved and refined in the space group C2/m by direct methods

$(TTP)TiCl_3$ (C_7H_8) (4). Small dark purple crystals were grown from pentane/toluene at −30 °C. A data set was collected, solved, and refined in the space group $P\bar{1}$ by direct methods.

$(DDP)ZrCl_3$ (5). Small almost colorless crystals were grown from pentane/toluene at −30 °C. A data set was collected, solved, and refined in the space group *Pnma* by direct methods.

$(TTP)Zr(CH_2Ph)_3$ (8). X-ray quality crystals were grown from toluene/pentane at −30 °C. A data set was collected, solved, and refined in the space group C2/c by direct methods.

$(TTP^*)Zr(CH_2Ph)_3$ (9). Large orange round X-ray quality crystals were grown from pentane/toluene at −30 °C. A data set was collected, solved, and refined in the space group $P\bar{1}$ by direct methods.

$(TTP)Zr(NMe_2)_3$ (10). Large yellow X-ray quality crystals were grown from pentane/toluene at −30 °C. A data set was collected and partially solved in the space group P1. An inversion center between the two independent molecules was observed. Its location was determined by calculating the difference of the absolute values of the x, y, and z coordinates for symmetrically related nitrogens. One of the two molecules was

then discarded and the origin redetermined. The space group was changed to $P\bar{1}$ and solved using direct methods.

(TTP)Ti(NMe$_2$)$_3$ (11). Large orange X-ray crystals were grown from pentane at –30 °C. A data set was collected, solved, and refined in the space group $P\bar{1}$ by direct methods.

(TP)$_2$Zr(NMe$_2$)$_2$ (13). Small yellow crystals were grown from pentane/toluene at –30 °C. A data set of strong reflections was collected, solved and refined in the space group $P2_1/c$ by direct methods.

(DDP)ZrCl(NMe$_2$)$_2$ (14). Small colorless crystals were grown from pentane at –30 °C. A data set was collected, solved, and refined in the space group $P\bar{1}$ by direct methods. There are two molecules in the unit cell.

Syntheses

Materials and General Considerations

For compounds **3-15**, all manipulations were performed using glove box, Schlenk or vacuum-line techniques. Argon and nitrogen were purified by passage through a column of MnO supported on silica. All solvents (except NMR solvents) were freshly distilled over sodium/benzophenone ketyl and were saturated with dinitrogen before use. Chloroform–d_1 was dried over 4 Å sieves. Benzene-d_6 was dried over 4 Å molecular sieves, and vacuum transferred to a sodium-mirrored air-free flask. Uncorrected melting points of crystalline samples in sealed capillaries (under argon) were reported. 2,4-pentadione, 3,5-bis(*tert*-butyl) phenol, and *p*-tolysulfonic acid were purchased from Aldrich and used as received. *p*-toluidine and 2,6-diisopropyl aniline were purchased from Aldrich, then sublimed and distilled respectively prior to use. ZrCl$_4$ and TiCl$_4$ were purchased from Aldrich. They were sublimed and distilled respectively prior to use. 3,5-

then discarded and the origin redetermined. The space group was changed to $P\bar{1}$ and solved using direct methods.

(TTP)Ti(NMe$_2$)$_3$ (11). Large orange X-ray crystals were grown from pentane at −30 °C. A data set was collected, solved, and refined in the space group $P\bar{1}$ by direct methods.

(TP)$_2$Zr(NMe$_2$)$_2$ (13). Small yellow crystals were grown from pentane/toluene at −30 °C. A data set of strong reflections was collected, solved and refined in the space group $P2_1/c$ by direct methods.

(DDP)2ZrCl(NMe$_2$)$_2$ (14). Small colorless crystals were grown from pentane at −30 °C. A data set was collected, solved, and refined in the space group $P\bar{1}$ by direct methods. There are two molecules in the unit cell.

Syntheses

Materials and General Considerations

For compounds 3-15, all manipulations were performed using glove box, Schlenk or vacuum-line techniques. Argon and nitrogen were purified by passage through a column of MnO supported on silica. All solvents (except NMR solvents) were freshly distilled over sodium\benzophenone ketyl and were saturated with dinitrogen before use. Chloroform-d_1 was dried over 4 Å sieves. Benzene-d_6 was dried over 4 Å molecular sieves, and vacuum transferred to a sodium-mirrored air-free flask. Uncorrected melting points of crystalline samples in sealed capillaries (under argon) were reported. 2,4-pentadione, 3,5-bis(*tert*-butyl) phenol, and *p*-tolylsulfonic acid were purchased from Aldrich and used as received. *p*-toluidine and 2,6-diisopropyl aniline were purchesed from Aldrich, then sublimed and distilled respectively prior to use. ZrCl$_4$ and TiCl$_4$ were purchased from Aldrich. They were sublimed and distilled respectively prior to use. 3,5-

di-*tert*-butylphenyl bromide[53], 3,5-di-*tert*-butylphenyl boronic acid[54] and 3,5-bis(3,5-di-*tert*-butylphenyl)-nitrobenzene[55] were prepared using literature methods. 3,5-bis(3,5-di-*tert*-butylphenyl)-aniline was prepared by reducing 3,5-bis(3,5-di-*tert*-butylphenyl)-nitrobenzene with two equivalents of Sn and an excess of concentrated HCl in refluxing thf. KOH was added and the solution was filtered to obtain the free base in 85% yield. $ZrCl_4(thf)_2$,[56] $TiCl_4(thf)_2$,[56] $Zr(CH_2Ph)_4$,[57] $Zr(NMe_2)_4$,[58] and $Ti(NMe_2)_4$[59] were prepared literature methods.

4-(3,5-bis(3,5-di-tert-butylphenyl)-phenylimino)-pent-4-en-2-one (2a). 2,4-pentadione (1.1 mL, 11 mmol), 3,5-bis(3,5-di-*tert*-butylphenyl)-aniline (4.61 g, 9.81 mmol), 60 mL of toluene, and *p*-tolylsulfonic acid (10 mg, 0.053 mmol) were placed into a 250 L round bottom flask fitted with a Dean-Stark apparatus. The reaction mixture was refluxed overnight with vigorous stirring. The solvent was removed under vacuum leaving a yellow solid (5.32 g, 98%). mp 220-223 °C. ^{1}H NMR ($CDCl_3$) δ 12.62 (s, 1 H, O*H*), δ 7.58 (s, 1 H, aromatic *H*), δ 7.46 (s, 2 H, aromatic *H*), δ 7.41 (s, 4 H, aromatic *H*), δ 7.27 (s, 1 H, aromatic *H*), δ 5.23 (s, 1 H, $CH_3C(NAr)CHC(OH)CH_3$), δ 2.12 (s, 3 H, $CH_{3\ \mathrm{backbone}}$), δ 2.09 (s, 3 H, $CH_{3\ \mathrm{backbone}}$), δ 1.36 (s, 36 H, $CH_{3\ \mathrm{t\text{-}vutyl}}$); $^{13}C\{^1H\}$ NMR ($CDCl_3$) δ ; EI/MS: M^+ m/z 551.3.

2-p-tolylamino-4-p-tolylimino-2-pentene (TTPH) (general method). 2,4-pentanedione, *p*-toluidine, and a very small amount of *p*-tolylsulfonic acid were heated at reflux overnight in toluene. The solvent was removed giving TTPH·(HCl). The free base was obtained by addition of KOH.

2-(2,6-diisopropyl)phenylamino-4-(2,6-diisopropyl)phenylimino-2-pentene (DDPH) (general method). 2,4-pentanedione (1 equiv) and 2,6-diisopropyl aniline (1 equiv) was

heated in a Dean Stark apparatus overnight in refluxing toluene. The solvent was removed giving the monodiketime DPH. DPH (1 equiv), 2,6-diisopropyl aniline (1 equiv) and *p*-tolylsulfonic acid (1 equiv) were heated in a Dean Stark apparatus overnight in refluxing toluene. The solvent was removed and KOH was added to give the free base DDPH. Very pure DDPH was obtained as long rods when recrystallized from pentane and a small amont of ethanol.

$(TTP)_2ZrCl_2$ (3). 5-mL of a toluene solution of Li(TTP) (1.55g, 5.45 mmol) was cooled to –78 °C, and added dropwise to a stirred suspension of $ZrCl_4(thf)_2$ (1.11g, 2.72 mmol) in 5 mL of toluene which was also at –78 °C. A yellow solid precipitated when the reaction mixture was allowed to warm to room temperature. The solution was filtered via cannula and the solid was extracted several times with hot toluene. The filtrates were combined, and the volume was reduced under vacuum and a yellow-green solid was recrystallized from toluene/pentane (0.98g, 50%). mp >250 °C. ^{1}H NMR ($CDCl_3$) δ 7.01 (d, J = 8.1Hz, 4 H, $C_6H_4CH_3$), δ 6.71 (br s, 4 H, $C_6\mathit{H}_4CH_3$), 5.34 (s, 1 H, $CH_3C(NAr)C\mathit{H}C(NAr)CH_3$), 2.28 (s, 6 H, $C_6H_4C\mathit{H}_3$), 1.63 (s, 6 H, $C\mathit{H}_3C(NAr)CHC(NAr)C\mathit{H}_3$); $^{13}C\{^1H\}$ NMR ($CDCl_3$) δ 166.29, 146.03, 135.11, 128.61, 127.73, 105.32, 25.12, 20.96. Anal.[50] Calcd for $C_{38}H_{42}N_4Cl_2Zr$: C, 63.66; H, 5.90; N, 7.81. Found: C, 63.70; H, 6.67; N, 7.78.

$(TTP)TiCl_3$ (4). Li(TTP) (1.43g, 5.03 mmol) dissolved in 10 mL of toluene was added to a stirred solution of $TiCl_4$(toluene) (2.6 mL of 1.82 mol/L, 0.47 mmol) at room temperature. The solution turned dark immediately upon addition and was slightly exothermic. The reaction mixture was allowed to stir for 2 h. The dark solution was removed via cannula and the remaining dark solid was extracted with hot toluene. The

filtrates were combined and their volume was reduced under vacuum. Dark purples were grown at –80 °C. (1.6 g, 84%). mp 125 °C. ^{1}H NMR ($CDCl_3$) δ 7.23-7.13 (mult, 8 H, $C_6\mathit{H}_4CH_3$); 6.03 (s, 1 H, $CH_3C(NAr)C\mathit{H}C(NAr)CH_3$); 2.36 (s, 6 H, $C_6H_4C\mathit{H}_3$); 2.12 (s, 6 H, $C\mathit{H}_3C(NAr)CHC(NAr)C\mathit{H}_3$); $^{13}C\{^1H\}$ NMR ($CDCl_3$) δ 159.82, 146.62, 129.73, 123.82, 104.86, 22.72, 21.12. Anal. Calcd for $C_{26}H_{29}N_2Cl_3Ti$: C, 59.62. H, 5.58; N, 5.35. Found: C, 59.29; H, 5.33, N, 5.22.

(DDP)ZrCl$_3$ (5). Li(DDP) (830 mg, 2.2 mmol) dissolved in 2 mL of toluene was added dropwise to a stirred suspension of $ZrCl_4$ (freshly sublimed) (500 mg, 2.1 mmol) in 2 mL of toluene. Several toluene washings (3 x 1 mL) were used to ensure complete Li(DDP) transfer. Once the addition was complete, the solution was allowed to stir overnight at 60 °C. The solution was removed via cannula while warm. The solvent was removed from the filtrate under vacuum. The remaining orange solid was recrystallized from CH_2Cl_2 at –80 °C yielding small slightly yellow crystals (670 mg, 50.7%). mp >220 °C. ^{1}H NMR ($CDCl_3$) δ 7.34-7.20 (m, 6 H, $C_6\mathit{H}_3(CH(CH_3)_2)$), 5.90 (s, 1 H, $CH_3C(NAr)C\mathit{H}C(NAr)CH_3$), 3.05 (septet, J_{HH} = 6.9, 4 H, $C_6H_3(C\mathit{H}(CH_3)_2)$), 1.94 (s, 6 H, $C\mathit{H}_3C(NAr)CHC(NAr)C\mathit{H}_3$), 1.37 (d, J_{HH} = 6.9, 12 H, $C_6H_3(CH(C\mathit{H}_3)_2)_2$), 1.18 (d, J_{HH} = 6.9, 12 H, $C_6H_3(CH(C\mathit{H}_3)_2)$; $^{13}C\{^1H\}$ NMR ($CDCl_3$) δ 171.3, 146.6, 141.7, 127.8, 124.6, 104.9, 29.1, 26.2, 24.7, 24.6; Anal.[50] Calcd for $C_{29}H_{41}N_2Cl_3Zr$: C, 56.53; H, 6.71; N, 4.54. Found: C, 56.54; H, 6.59; N, 4.42.

(DDP)ZrCl$_3$(thf) (6). Li(DDP) (450 mg, 1.15 mmol) dissolved in 2 mL of toluene was added dropwise to a stirred suspension of $ZrCl_4(thf)_2$ (430 mg, 1.14 mmol) in 2 mL of toluene at room temperature. Several toluene washings (3 x 1 mL) were used to ensure

good Li(DDP) transfer. After the addition was complete, the solution was allowed to stir overnight. The clear orange solution was filtered off via cannula. The volume of solution was reduced under vacuum and then cooled to –80 °C yielding small yellow crystals (390 mg, 49%). mp >225 °C. ^1H NMR (C_6D_6) δ 7.15 (s, 6 H, $C_6\mathit{H_3}(CH(CH_3)_2)_2$), 5.43 (s, 1 H, $CH_3C(NAr)C\mathit{H}C(NAr)CH_3$), 3.90 (mult, 4 H, *thf*), 3.58 (septet, J_{HH} = 6.8, 4 H, $C_6H_3((C\mathit{H}(CH_3)_2)_2)$, 1.65 (s, 6 H, $C\mathit{H_3}C(NAr)CHC(NAr)C\mathit{H_3})$)), 1.54 (d, J_{HH} = 6.8, 12 H, $C_6H_3(CH(C\mathit{H_3})_2)_2$), 1.10 (d, J_{HH} = 6.8, 12 H, $C_6H_3(CH(C\mathit{H_3})_2)_2$), 1.05 (mult, 4 H, *thf*); $^{13}C\{^1H\}$ NMR (C_6H_6) δ 169.33, 145.86, 144.08, 124.76, 105.64, 77.00, 28.93, 26.45, 25.66, 24.82, 24.74;

(DDP)TiCl$_3$ (7). Li(DDP) (300g, 0.9 mmol) dissolved in 2 mL of toluene was added dropwise to $TiCl_4(thf)_2$ (380mg, 0.9 mmol) in 2 mL of toluene at –78 °C. Upon addition, the solution turned dark. The reaction mixture was allowed to warm to RT and stir overnight. The solution was removed via filter stick. The remaining dark sticky substance was pumped on yielding a flaky dark solid. Purifying the product further proved difficult; ^1H NMR ($CDCl_3$) δ 7 (m, 6 H, $C_6\mathit{H_3}(CH(CH_3)_2)_2$), 6.26 (s, 1 H, $CH_3C(NAr)C\mathit{H}C(NAr)CH_3$), 2.97 (septet, J_{HH} = 6.6, 4 H, $C_6H_3(C\mathit{H}(CH_3)_2)_2$), 2.00 (s, 6 H, $C\mathit{H_3}C(NAr)CHC(NAr)C\mathit{H_3}$), 1.33 (d, J_{HH} = 6.6, 12 H, $C_6H_3(CH(C\mathit{H_3})_2)_2$))), 1.11 (d, J_{HH} = 6.6, 12 H, $C_6H_3(CH(C\mathit{H_3})_2)_2$).

(TTP)Zr(CH$_2$Ph)$_3$ (8). TTPH (1.97g, 7.08 mmol) dissolved in 20 mL of toluene was added dropwise to a stirred solution of $Zr(CH_2Ph)_4$ (3.21g, 7.05 mmol) dissolved in 5 mL of toluene. The reaction mixture was allowed to stir for 8 hours. The volume was reduced under vacuum and the solution was placed in the –80 °C freezer. A yellow solid

precipitated. (3.55g, 78%). mp[50] 98-100 °C. ^1H *NMR* (C_6D_6) δ 7.10 (mult, 6 H, aromatic), 6.90 (mult, 7 H, aromatic), 6.73 (mult, 10 H, aromatic), 5.06 (s, 1 H, $CH_3C(NAr)C\mathit{H}C(NAr)CH_3$), 2.61 (s, 6H, $C\mathit{H}_2C_6H_5$), 2.09 (s, 6 H, $C_6H_4C\mathit{H}_3$), 1.62 (s, 6 H, $C\mathit{H}_3C(NAr)CHC(NAr)C\mathit{H}_3$); $^{13}C\{^1H\}$ NMR (C_6D_6) δ 160.58, 146.68, 143.52, 135.63, 130.02, 128.77, 127.65, 126.03, 121.84, 102.14, 75.62, 22.76, 20.84. Anal.[50] Calcd for $C_{40}H_{42}N_2Zr$: C, 74.83; H, 6.59; N, 4.36. Found: C, 74.44; H, 6.56; N, 4.60.

(TTP*)Zr(CH$_2$Ph)$_2$ (9). (TTP)Zr(CH_2Ph)$_3$ (1.1 g, 1.7 mmol) was dissolved in 5 mL of toluene and heated at 45 °C for 48 hours. The solvent was removed under vacuum. Orange-yellow crystals were obtained from toluene/pentane (1:1) at –30 °C (0.64 g, 68%). mp 140-142 °C. ^1H NMR (C_6D_6) δ 7.80 (mult, 1 H, aromatic), 7.18-6.75 (mult, 13 H, aromatic), 6.48 (d, J = 9.0 Hz, 4 H, aromatic), 5.31 (s, 1 H, $CH_3C(NAr)C\mathit{H}C(NAr)CH_3$), 2.33 (s, 3 H, $C_6H_4C\mathit{H}_3$), 2.13 (d, J = 9.6 Hz, 2 H, $C\mathit{H}_2C_6H_5$), 2.13 (s, 3 H, $C_6H_4C\mathit{H}_3$), 2.07 (s, 3H, $C\mathit{H}_{3\ \mathrm{backbone}}$), 1.66 (d, J = 9.6 Hz, 2 H, $C\mathit{H}_2C_6H_5$), 1.58 (s, 3 H, $C\mathit{H}_{3\ \mathrm{backbone}}$); $^{13}C\{^1H\}$ NMR (C_6H_6) δ 186.86, 159.11, 158.52, 141.80, 138.85, 137.45, 132.63, 130.44, 129.96, 129.84, 129.26, 128.17, 122.90, 118.71, 106.46, 66.62, 24.62, 24.23, 21.60, 20.90; Anal.[50] Calcd for $C_{33}H_{34}N_2Zr$: C, 72.08; H, 6.23; N, 5.09. Found: C, 71.90; H, 6.46; N, 4.70.

(TTP)Zr(NMe$_2$)$_3$ (10). TTPH (1.30g, 0.467 mmol) dissolved in 2 mL of toluene was added dropwise to a stirred solution of $Zr(NMe_2)_4$ (1.25g, 0.467 mmol) dissolved in 2 mL of toluene at room temperature. After stirring for 1 hour, the toluene was removed under vacuum leaving an orange-yellow solid (2.26g, 98%). mp 117-119 °C. ^1H NMR (C_6D_6) δ 6.98 (d, J = 8 Hz, 4 H, $C_6\mathit{H}_4CH_3$), 6.76 (d, J = 8 Hz, 4 H, $C_6\mathit{H}_4CH_3$), 5.10 (s, 1 H,

$CH_3C(NAr)C\mathit{H}C(NAr)CH_3$), 2.80 (s, 18 H, $N(C\mathit{H}_3)_2$), 2.12 (s, 6 H, $C_6H_4C\mathit{H}_3$), 1.75(s, 6 H, $C\mathit{H}_3C(NAr)CHC(NAr)C\mathit{H}_3$); $^{13}C\{^1H\}$ NMR (C_6H_6) δ 164.54, 148.26, 133.04, 129.15, 125.08, 100.23, 42.41, 24.21, 20.84. Anal.[50] Calcd for $C_{25}H_{39}N_5Zr$: C, 59.95; H, 7.85; N, 13.98. Found: C, 59.59; H, 7.48; N, 13.89.

(TTP)Ti(NMe$_2$)$_3$ (11). TTPH (3.8g, 13.8 mmol) in 5mL of toluene was added dropwise to a stirred solution of $Ti(NMe_2)_4$ (3.36g, 13.8 mmol) at room temperature. The reaction mixture was heated at 35 °C overnight. The toluene was removed under vacuum. Orange crystals formed from pentane at –80 °C. (5.5g, 87%). mp 140-143 °C. ^1H NMR (C_6D_6) δ 6.95 (d, J = 9 Hz, 4 H, $C_6\mathit{H}_4CH_3$) 6.65 (d, J = 9.0 Hz, 4 H, $C_6\mathit{H}_4CH_3$), 5.21 (s, 1 H, $CH_3C(NAr)C\mathit{H}C(NAr)CH_3$), 2.95 (s, 18 H, $N(C\mathit{H}_3)_2$), 2.13 (s, 6 H, $C_6H_4C\mathit{H}_3$), 1.78 (s, 6 H, $C\mathit{H}_3C(NAr)CHC(NAr)C\mathit{H}_3$); $^{13}C\{^1H\}$ NMR (C_6D_6) δ 162.81, 150.16, 132.28, 128.57, 124.70, 100.24, 46.23, 24.43, 20.84; Anal. Calcd for $C_{25}H_{39}N_5Ti$: C, 65.63; H, 8.59; N, 15.31. Found: C, 65.70; H, 8.75, N, 15.01.

(TTP)$_2$Zr(NMe$_2$)$_2$ (12). TTPH (2.1 g, 7.5 mmol) dissolved in 5 mL of toluene was added dropwise to a stirred solution of $Zr(NMe_2)_4$ (1.01 g, 3.8 mmol) dissolved in 5 mL. The solution was allowed to stir for 5 hours at reflux. The toluene was removed under vacuum and the solid was recrystallized from pentane yielding orange-yellow crystals (1.6 g, 57.8%). mp 190 – 195 °C. ^1H NMR (C_6D_6) δ 7.25 (br s, 2 H, $C_6\mathit{H}_4CH_3$), 7.07 (mult, 2 H, $C_6\mathit{H}_4CH_3$), 6.87 (mult, 3 H, $C_6\mathit{H}_4CH_3$), 5.67 (d, J = 3 Hz, 1 H, $C_6\mathit{H}_4CH_3$), 5.13 (s, 1H, $CH_3C(NAr)C\mathit{H}C(NAr)CH_3$), 2.64 (broad s, 6 H, $N(C\mathit{H}_3)_2$), 2.22 (s, 3 H, $C_6H_4C\mathit{H}_3$), 2.06 (s, 3 H, $C_6H_4C\mathit{H}_3$) , 1.77 (s, 3 H, $C\mathit{H}_3C(NAr)CHC(NAr)CH_3$), 1.43 (s, 3 H, $CH_3C(NAr)CHC(NAr)C\mathit{H}_3$). $^{13}C\{^1H\}$ NMR (C_6H_6) δ 164.90, 164.33, 150.35, 149.99,

$CH_3C(NAr)CHC(NAr)CH_3$), 2.80 (s, 18 H, $N(CH_3)_2$), 2.12 (s, 6 H, $C_6H_4CH_3$), 1.75(s, 6 H, $CH_3C(NAr)CHC(NAr)CH_3$). $^{13}C\{^1H\}$ NMR (C_6H_6) δ 164.54, 148.26, 133.04, 129.15, 125.08, 100.23, 42.41, 24.21, 20.84. Anal.[50] Calcd for $C_{25}H_{40}N_5Zr$: C, 59.95; H, 7.85; N, 13.98. Found: C, 59.59; H, 7.48; N, 13.89

$(TTP)Ti(NMe_2)_3$ (11). TTPH (3.5g, 13.8 mmol) in 5mL of toluene was added dropwise to a stirred solution of $Ti(NMe_2)_4$ (3.06g, 13.8 mmol) at room temperature. The reaction mixture was heated at 35 °C overnight. The toluene was removed under vacuum. Orange crystals formed from pentane at -80 °C (5.5g, 87%), mp 140-143 °C. ^1H NMR (C_6D_6) δ 6.95 (d, J = 9 Hz, 4 H, $C_6H_4CH_3$) 6.65 (d, J = 9.0 Hz, 4 H, $C_6H_4CH_3$), 5.21 (s, 1 H, $CH_3C(NAr)CHC(NAr)CH_3$), 2.99 (s, 18 H, $N(CH_3)_2$), 2.13 (s, 6 H, $C_6H_4CH_3$), 1.78 (s, 6 H, $CH_3C(NAr)CHC(NAr)CH_3$). $^{13}C\{^1H\}$ NMR (C_6D_6) δ 162.81, 150.16, 132.28, 128.57, 124.70, 100.24, 46.23, 24.45, 20.84. Anal. Calcd for $C_{25}H_{40}N_5Ti$: C, 65.63; H, 8.59; N, 15.31. Found: C, 65.70; H, 8.75; N, 15.01

$(TTP)_2Zr(NMe_2)_2$ (12). TTPH (2.1 g, 7.5 mmol) dissolved in 5 mL of toluene was added dropwise to a stirred solution of $Zr(NMe_2)_4$ (1.01 g, 3.8 mmol) dissolved in 5 mL. The solution was allowed to stir for 5 hours at reflux. The toluene was removed under vacuum and the solid was recrystallized from pentane yielding orange-yellow crystals (1.6 g, 57.8%); mp 190 – 195 °C. ^1H NMR (C_6D_6) δ 7.25 (br s, 2 H, $C_6H_4CH_3$), 7.07 (mult, 2 H, $C_6H_4CH_3$), 6.87 (mult, 3 H, $C_6H_4CH_3$), 5.65 (d, J = 3 Hz, 1 H, $C_6H_4CH_3$), 5.13 (s, 1H, $CH_3C(NAr)CHC(NAr)CH_3$), 2.64 (broad s, 6 H, $N(CH_3)_2$), 2.22 (s, 3 H, $C_6H_4CH_3$), 2.06 (s, 3 H, $C_6H_4CH_3$), 1.77 (s, 3 H, $CH_3C(NAr)CHC(NAr)CH_3$), 1.43 (s, 3 H, $CH_3C(NAr)CHC(NAr)CH_3$). $^{13}C\{^1H\}$ NMR (C_6H_6) δ 164.90, 164.03, 150.35, 149.99, 133.78, 133.07, 128.93, 128.47, 128.42, 127.20, 125.78, 100.50, 46.45, 25.81, 25.58, 20.96, 20.85. Anal.[50] Calcd for $\mathrm{C_{42}H_{54}N_6Zr}$: C, 68.74; H, 7.36; N, 11.44. Found: C, 68.97; H, 7.35; N, 10.70.

$\mathbf{(TP)_2Zr(NMe_2)_2}$ (13). TPH (370 mg, 1.90 mmol) dissolved in 20 mL of pentane was added dropwise to a stirred solution of $\mathrm{Zr(NMe_2)_4}$ (260 mg, 0.97 mmol) dissolved in 2 mL of pentane at room temperature. Upon completion of the addition, a yellow solid precipitated. The solid was allowed to settle and the solution was removed via cannula. The solid was pure by ^{1}H NMR, but could be recrystallized from pentane if necessary. The volume of the filtrate was reduced under vacuum and placed in –80 °C freezer to yield several more crops of yellow crystals (355mg, 66%). mp 164-166 °C. ^{1}H NMR ($\mathrm{C_6D_6}$) δ 6.97 (s, 2 H, $\mathrm{C_6}\mathit{H_4}\mathrm{CH_3}$), 6.94 (s, 1 H, $\mathrm{C_6}\mathit{H_4}\mathrm{CH_3}$), 6.66 (s, 1 H, $\mathrm{C_6}\mathit{H_4}\mathrm{CH_3}$), 4.95 (s, 1 H, $\mathrm{CH_3C(O)C}\mathit{H}\mathrm{C(NAr)CH_3}$), 3.30 (s, 6 H, $\mathrm{N(C}\mathit{H_3}\mathrm{)_2}$), 2.16 (s, 3 H, $\mathrm{C_6H_4C}\mathit{H_3}$), 1.56 (s, 3 H, $\mathrm{C}\mathit{H_3}{}_{\text{ backbone}}$), 1.42 (s, 3 H, $\mathrm{C}\mathit{H_3}{}_{\text{ backbone}}$); ^{13}C{^{1}H} NMR ($\mathrm{C_6D_6}$) δ 173.90, 168.91, 148.26, 133.19, 129.15, 128.87, 124.46, 123.41, 102.78, 44.56, 24.41, 23.39, 20.83; Anal. Calcd for $\mathrm{C_{28}H_{40}N_4O_2Zr}$: C, 60.50; H, 7.25; N, 10.08. Found: C, 60.0; H, 7.39; N, 9.90.

$\mathbf{(DDP)ZrCl(NMe_2)_2}$ (14). A stirred suspension of DDPH(HCl) (430 mg, 0.94 mmol) dissolved in 2 mL toluene was cooled to –78 °C. $\mathrm{Zr(NMe_2)_4}$ (250 mg, 0.93 mmol) dissolved in 2 mL of toluene was added dropwise to the cooled solution via cannula. Once the addition was complete, the solution was allowed to warm to RT. All solids dissolved leaving a clear green solution. The reaction mixture was allowed to stir overnight. The toluene was removed under vacuum. The remaining solid was recrystallized from pentane yielding small colorless crystals (300 mg, 51%). mp 197-199

°C. ^{1}H NMR (C_6D_6) at 50 °C δ 7.12 (s, 6 H, $C_6\mathit{H}_3(CH(CH_3)_2)_2$), 5.20 (s, 1 H, $CH_3C(NAr)C\mathit{H}C(NAr)CH_3$), 3.03 (sept, *J* = 6.9 Hz, 4 H, $C_6H_3(C\mathit{H}(CH_3)_2)_2$), 2.70 (s, 12 H, $N(C\mathit{H}_3)_2$), 1.63 (s, 6 H, $C\mathit{H}_3C(NAr)CHC(NAr)C\mathit{H}_3$), 1.37 (d, *J* = 6.8 Hz, 12 H, $C_6H_3(CH(C\mathit{H}_3)_2)_2$), 1.15 (d, *J* = 6.8, 12 H, $C_6H_3(CH(C\mathit{H}_3)_2)_2$), $^{13}C\{^{1}H\}$ NMR (C_6D_6) at 50 °C δ 167.02, 149.29, 141.69, 126.05, 123.90, 100.84, 41.73, 29.104, 25.95, 25.13, 24.27. Anal.[50] Calcd for $C_{33}H_{53}N_4ClZr$: C, 62.58; H, 8.45; N, 8.85. Found: C, 62.50; H, 8.61; N, 8.62.

(TTP)Zr(NMe$_2$)(*p*-NC$_6$H$_4$Me) (15). *p*-toluidine (69 mg, 0.64 mmol) was added dropwise at RT to a stirred solution of (TTP)Zr(NMe$_2$)$_3$ (320 mg, 0.63 mmol) dissolved in 2 mL of toluene The reaction mixture was allowed to stir for 6 hours. The solution volume was reduced under vacuum. The yellow solid was washed with toluene and then pentane. Due to poor solubility, recrystallization as well as collection of ^{13}C NMR data has been unsuccessful. (mp 210-213 °C). ^{1}H NMR (C_6D_6) δ 6.91 (d, *J* = 7.8 Hz, 6 H, aromatic) 6.74 (d, *J* = 8.1 Hz, 4 H, aromatic), 6.36 (d, *J* = 8.1 Hz, 2 H, aromatic), 5.30 (s, 1H, $CH_3C(NAr)C\mathit{H}C(NAr)CH_3$), 2.78 (s, 6H, $N(C\mathit{H}_3)_2$), 2.26 (s, 3 H. $NC_6H_4C\mathit{H}_3$), 2.11 (s, 6 H, $C_6H_4C\mathit{H}_3$), 1.82 (s, 6 H, $C\mathit{H}_3C(NAr)CHC(NAr)C\mathit{H}_3$).

Appendix A: Bond Lengths and Angles

for

(TTP)$_2$ZrCl$_2$ (**3**)
(TTP)TiCl$_3$ (**4**)
(DDP)ZrCl$_3$ (**5**)
(TTP)Zr(CH$_2$Ph)$_3$ (**8**)
(TTP*)Zr(CH$_2$Ph)$_2$ (**9**)
(TTP)Zr(NMe$_2$)$_3$ (**10**)
(TTP)Ti(NMe$_2$)$_3$ (**11**)
(TP)$_2$Zr(NMe$_2$)$_2$ (**13**)
(DDP)ZrCl(NMe$_2$)$_2$ (**14**)

Table 6 Selected Bond Lengths and Angles for 3,4 and 5

$(TTP)_2ZrCl_2$ (3)		$(TTP)TiCl_3$ (4)		$(DDP)ZrCl_3$ (5)	
		Bond Lengths (Å)			
Zr(1)-N(1)	2.243(2)	Ti(1)-N(2)	1.995(4)	Zr(1)-N(1)#1	2.202(2)
Zr(1)-N(2)	2.197(2)	Ti(1)-N(1)	1.995(4)	Zr(1)-N(1)	2.202(2)
Zr(1)-N(3)	2.214(2)	Ti(1)-Cl(1)	2.218(2)	Zr(1)-Cl(1)	2.3945(7)
Zr(1)-N(4)	2.272(2)	Ti(1)-Cl(2)	2.337(2)	Zr(1)-Cl(1)#1	2.3945(7)
Zr(1)-Cl(1)	2.4312(7)	Ti(1)-Cl(3)	2.335(2)	Zr(1)-Cl(2)	2.3392(9)
Zr(1)-Cl(2)	2.4426(7)	Ti(1)-C(4)	2.535(5)		
		Ti(1)-C(3)	2.535(4)		
		Ti(1)-C(2)	2.559(5)		
		Bond Angles (°)			
N(2)-Zr(1)-N(3)	157.65(6)	N(2)-Ti(1)-N(1)	85.1(2)	N(1)#1-Zr(1)-N(1)	83.64(8)
N(2)-Zr(1)-N(1)	79.31(7)	N(2)-Ti(1)-Cl(1)	95.38(12)	N(1)#1-Zr(1)-Cl(2)	102.54(5)
N(3)-Zr(1)-N(1)	87.49(6)	N(1)-Ti(1)-Cl(1)	99.29(12)	N(1)-Zr(1)-Cl(2)	102.54(5)
N(2)-Zr(1)-N(4)	83.19(6)	N(2)-Ti(1)-Cl(3)	162.77(12)	N(1)#1-Zr(1)-Cl(1)	149.45(5)
N(3)-Zr(1)-N(4)	78.52(6)	N(1)-Ti(1)-Cl(3)	91.27(13)	N(1)-Zr(1)-Cl(1)	86.97(4)
N(1)-Zr(1)-N(4)	88.72(6)	Cl(1)-Ti(1)-Cl(3)	101.83(6)	Cl(2)-Zr(1)-Cl(1)	107.86(3)
N(2)-Zr(1)-Cl(1)	99.64(5)	N(2)-Ti(1)-Cl(2)	87.25(12)	N(1)#1-Zr(1)-Cl(1)#	186.97(4)
N(3)-Zr(1)-Cl(1)	97.67(5)	N(1)-Ti(1)-Cl(2)	152.34(12)	N(1)-Zr(1)-Cl(1)#1	149.46(5)
N(1)-Zr(1)-Cl(1)	87.39(5)	Cl(1)-Ti(1)-Cl(2)	107.87(6)	Cl(2)-Zr(1)-Cl(1)#1	107.86(3)
N(4)-Zr(1)-Cl(1)	174.67(4)	Cl(3)-Ti(1)-Cl(2)	88.27(7)	Cl(1)-Zr(1)-Cl(1)#1	86.54(4)
N(2)-Zr(1)-Cl(2)	98.70(5)				
N(3)-Zr(1)-Cl(2)	95.28(5)				
N(1)-Zr(1)-Cl(2)	176.51(5)				
N(4)-Zr(1)-Cl(2)	93.91(5)				
Cl(1)-Zr(1)-Cl(2)	90.13(3)				

Table 7 Selected Bond Lengths and Angles for 8 and 9

$(TTP)Zr(CH_2Ph)_3$ (8)		$(TTP^*)Zr(CH_2Ph)_2$ (9)	
Bond Lengths (Å)			
Zr(1)-N(2)	2.189(2)	Zr(1)-N(1)	2.175(2)
Zr(1)-N(1)	2.205(2)	Zr(1)-N(2)	2.253(2)
Zr(1)-C(20)	2.253(3)	Zr(1)-C(14)	2.260(2)
Zr(1)-C(27)	2.304(3)	Zr(1)-C(27)	2.288(2)
Zr(1)-C(34)	2.313(3)	Zr(1)-C(20)	2.302(2)
		Zr(1)-C(21)	2.584(2)
		Zr(1)-C(13)	2.781(2)
Bond Angles (°)			
N(2)-Zr(1)-N(1)	76.51(8)	N(1)-Zr(1)-N(2)	77.91(6)
N(2)-Zr(1)-C(20)	111.35(11)	N(1)-Zr(1)-C(14)	138.48(6)
N(1)-Zr(1)-C(20)	112.51(10)	N(2)-Zr(1)-C(14)	60.63(7)
N(2)-Zr(1)-C(27)	84.79(9)	N(1)-Zr(1)-C(27)	100.45(7)
N(1)-Zr(1)-C(27)	133.30(9)	N(2)-Zr(1)-C(27)	114.65(6)
C(20)-Zr(1)-C(27)	114.13(11)	C(14)-Zr(1)-C(27)	98.65(7)
N(2)-Zr(1)-C(34)	139.09(10)	N(1)-Zr(1)-C(20)	98.92(7)
N(1)-Zr(1)-C(34)	81.81(10)	N(2)-Zr(1)-C(20)	116.16(6)
C(20)-Zr(1)-C(34)	108.90(12)	C(14)-Zr(1)-C(20)	97.54(7)
C(27)-Zr(1)-C(34)	85.48(11)	C(27)-Zr(1)-C(20)	128.25(7)
C(21)-C(20)-Zr(1)	99.1(2)	N(1)-Zr(1)-C(21)	113.00(6)
C(28)-C(27)-Zr(1)	117.6(2)	N(2)-Zr(1)-C(21)	147.23(6)
C(35)-C(34)-Zr(1)	110.7(2)	C(14)-Zr(1)-C(21)	101.84(7)
		C(27)-Zr(1)-C(21)	94.32(6)
		C(20)-Zr(1)-C(21)	34.13(6)
		N(1)-Zr(1)-C(13)	108.35(6)
		N(2)-Zr(1)-C(13)	30.56(5)
		C(14)-Zr(1)-C(13)	30.13(6)
		C(27)-Zr(1)-C(13)	110.53(6)
		C(20)-Zr(1)-C(13)	107.90(7)
		C(21)-Zr(1)-C(13)	126.22(6)
		C(21)-C(20)-Zr(1)	83.58(11)
		C(28)-C(27)-Zr(1)	99.64(11)

Table 8 Selected Bond Lengths and Angles for 10 and 11

(TTP)Zr(NMe$_2$)$_3$ (10)		(TTP)Ti(NMe$_2$)$_3$ (11)	
	Bond Lengths (Å)		
Zr(1)-N(3)	2.019(4)	Ti(1)-N(4)	1.9102(13)
Zr(1)-N(4)	2.031(4)	Ti(1)-N(5)	1.9180(13)
Zr(1)-N(5)	2.071(4)	Ti(1)-N(3)	1.9592(13)
Zr(1)-N(2)	2.211(4)	Ti(1)-N(1)	2.0900(12)
Zr(1)-N(1)	2.350(4)	Ti(1)-N(2)	2.2371(13)
	Bond Angles (°)		
N(3)-Zr(1)-N(4)	120.5(2)	N(4)-Ti(1)-N(5)	121.34(6)
N(3)-Zr(1)-N(5)	94.5(2)	N(4)-Ti(1)-N(3)	92.71(6)
N(4)-Zr(1)-N(5)	91.6(2)	N(5)-Ti(1)-N(3)	91.49(6)
N(3)-Zr(1)-N(2)	118.4(2)	N(4)-Ti(1)-N(1)	119.35(6)
N(4)-Zr(1)-N(2)	119.8(2)	N(5)-Ti(1)-N(1)	118.34(5)
N(5)-Zr(1)-N(2)	95.0(2)	N(3)-Ti(1)-N(1)	95.65(5)
N(3)-Zr(1)-N(1)	92.3(2)	N(4)-Ti(1)-N(2)	89.48(6)
N(4)-Zr(1)-N(1)	88.2(2)	N(5)-Ti(1)-N(2)	88.29(5)
N(5)-Zr(1)-N(1)	172.13(14)	N(3)-Ti(1)-N(2)	177.56(5)
N(2)-Zr(1)-N(1)	78.28(14)	N(1)-Ti(1)-N(2)	82.32(5)
C(20)-N(3)-C(21)	112.0(5)	C(21)-N(3)-C(20)	108.9(2)
C(20)-N(3)-Zr(1)	126.5(4)	C(21)-N(3)-Ti(1)	124.95(13)
C(21)-N(3)-Zr(1)	121.3(4)	C(20)-N(3)-Ti(1)	125.17(12)
C(22)-N(4)-C(23)	113.8(5)	C(23)-N(4)-C(22)	112.2(2)
C(22)-N(4)-Zr(1)	132.0(4)	C(23)-N(4)-Ti(1)	123.55(14)
C(23)-N(4)-Zr(1)	114.1(4)	C(22)-N(4)-Ti(1)	124.3(2)
C(24)-N(5)-C(25)	107.6(4)	C(24)-N(5)-C(25)	112.4(2)
C(24)-N(5)-Zr(1)	127.9(3)	C(24)-N(5)-Ti(1)	129.4(2)
C(25)-N(5)-Zr(1)	123.8(3)	C(25)-N(5)-Ti(1)	118.09(12)

Table 9 Selected Bond Lengths and Angles for 13

$(TP)_2Zr(NMe_2)_2$ (13)	
Bond Lengths (Å)	
Zr(1)-O(2)	2.050(4)
Zr(1)-O(1)	2.051(4)
Zr(1)-N(4)	2.077(5)
Zr(1)-N(3)	2.076(5)
Zr(1)-N(1)	2.385(5)
Zr(1)-N(2)	2.400(5)
Bond Angles (°)	
O(2)-Zr(1)-O(1)	164.0(2)
O(2)-Zr(1)-N(4)	95.7(2)
O(1)-Zr(1)-N(4)	94.7(2)
O(2)-Zr(1)-N(3)	94.5(2)
O(1)-Zr(1)-N(3)	94.6(2)
N(4)-Zr(1)-N(3)	104.4(2)
O(2)-Zr(1)-N(1)	90.7(2)
O(1)-Zr(1)-N(1)	76.4(2)
N(4)-Zr(1)-N(1)	164.7(2)
N(3)-Zr(1)-N(1)	88.9(2)
O(2)-Zr(1)-N(2)	77.0(2)
O(1)-Zr(1)-N(2)	91.6(2)
N(4)-Zr(1)-N(2)	86.3(2)
N(3)-Zr(1)-N(2)	167.1(2)
N(1)-Zr(1)-N(2)	81.6(2)
C(26)-N(3)-C(25)	109.7(5)
C(26)-N(3)-Zr(1)	123.0(4)
C(25)-N(3)-Zr(1)	126.9(4)
C(27)-N(4)-C(28)	110.0(5)
C(27)-N(4)-Zr(1)	125.0(4)
C(28)-N(4)-Zr(1)	124.2(4)

Table 10 Selected Bond Lengths and Angles for 14

(DDP)ZrCl(NMe$_2$)$_2$ #1 (14)		**(DDP)ZrCl(NMe$_2$)$_2$ #2**	
Bond Lengths (Å)			
Zr(1)-N(4)	2.014(2)	Zr(11)-N(13)	2.014(2)
Zr(1)-N(3)	2.052(2)	Zr(11)-N(14)	2.066(2)
Zr(1)-N(2)	2.249(2)	Zr(11)-N(11)	2.258(2)
Zr(1)-N(1)	2.319(2)	Zr(11)-N(12)	2.328(2)
Zr(1)-Cl(1)	2.4776(8)	Zr(11)-Cl(11)	2.4979(8)
Bond Angles (°)			
N(4)-Zr(1)-N(3)	107.28(11)	N(13)-Zr(11)-N(14)	107.66(10)
N(4)-Zr(1)-N(2)	101.97(9)	N(13)-Zr(11)-N(11)	101.52(9)
N(3)-Zr(1)-N(2)	93.92(9)	N(14)-Zr(11)-N(11)	92.01(9)
N(4)-Zr(1)-N(1)	103.77(9)	N(13)-Zr(11)-N(12)	101.56(9)
N(3)-Zr(1)-N(1)	148.94(10)	N(14)-Zr(11)-N(12)	150.75(9)
N(2)-Zr(1)-N(1)	80.61(8)	N(11)-Zr(11)-N(12)	80.60(8)
N(4)-Zr(1)-Cl(1)	104.61(7)	N(13)-Zr(11)-Cl(11)	107.71(8)
N(3)-Zr(1)-Cl(1)	86.57(8)	N(14)-Zr(11)-Cl(11)	87.65(7)
N(2)-Zr(1)-Cl(1)	151.99(6)	N(11)-Zr(11)-Cl(11)	149.42(6)
N(1)-Zr(1)-Cl(1)	84.63(6)	N(12)-Zr(11)-Cl(11)	84.88(6)
C(30)-N(3)-C(31)	110.7(3)	C(133)-N(13)-C(132)	112.5(3)
C(30)-N(3)-Zr(1)	128.8(2)	C(133)-N(13)-Zr(11)	125.5(2)
C(31)-N(3)-Zr(1)	120.3(2)	C(132)-N(13)-Zr(11)	121.8(2)
C(33)-N(4)-C(32)	111.8(3)	C(130)-N(14)-C(131)	111.6(3)
C(33)-N(4)-Zr(1)	124.5(2)	C(130)-N(14)-Zr(11)	116.5(2)
C(32)-N(4)-Zr(1)	123.5(2)	C(131)-N(14)-Zr(11)	131.9(2)

Appendix B: Single Crystal X-ray Structure Key Data Collection and Refinement Parameters

$(TTP)_2ZrCl_2$ (**3**)
$(TTP)TiCl_3$ (**4**)
$(DDP)ZrCl_3$ (**5**)
$(TTP)Zr(CH_2Ph)_3$ (**8**)
$(TTP^*)Zr(CH_2Ph)_2$ (**9**)
$(TTP)Zr(NMe_2)_3$ (**10**)
$(TTP)Ti(NMe_2)_3$ (**11**)
$(TP)_2Zr(NMe_2)_2$ (**13**)
$(DDP)ZrCl(NMe_2)_2$ (**14**)

Table 11 Key X-ray Parameters, Refinement and Results for 3, 4 and 5

	$(TTP)_2ZrCl_2$ (3)	**$(TTP)TiCl_3$ (4)**	**$(DDP)ZrCl_3$ (5)**
Empirical formula	$C_{38}H_{42}Cl_2N_4Zr$	$C_{19}H_{21}Cl_3N_2Ti(C_7H_8)$	$C_{29}H_{41}Cl_3N_2Zr$
Formula weight	716.88	503.69	615.21
Temperature (K)	173(2)	173(2)	173(2)
Wavelength (Å)	0.71073	0.71073	0.71073
Crystal system	Monoclinic	Triclinic	Orthorhombic
Space group	$P2_1/n$	$P\bar{1}$	*P*nma
Cell			
a (Å)	9.179(2)	7.286(2)	14.054(3)
b (Å)	22.868(5)	13.154(3)	21.842(4)
c (Å)	16.813(3)	15.253(3)	9.856(2)
α (°)	90	103.25(3)	90
β (°)	98.77(3)	99.96(3)	90
χ (°)	90	94.58(3)	90
Volume (Å^3)	3487.9(12)	1390.6(5)	3025.6(11)
Z	4	2	4
d (calc.) (Mg/m^3)	1.365	1.203	1.351
Abs. coef. (mm^{-1})	0.501	0.609	0.648
F(000)	1488	516	1280
Crystal size (mm)	0.2 x 0.2 x 0.25	0.2 x 0.2 x 0.25	0.2 x 0.1 x 0.06
2θ range (°)	1.51 to 28.39	1.60 to 28.29	1.86 to 28.32
Index ranges	$-10 <= h <= 12$ $-27 <= k <= 30$ $-22 <= l <= 21$	$-9 <= h <= 9$ $-17 <= k <= 17$ $-13 <= l <= 20$	$-18 <= h <= 18$ $-28 <= k <= 29$ $-12 <= l <= 12$
Reflections collected	21485	8178	33445
Independent reflections	8272 [*R*(int) = 0.0318]	5865 [*R*(int) = 0.0903]	3804 [*R*(int) = 0.0437]
Refinement method	Full-matrix least-squares on F^2	Full-matrix least-squares on F^2	Full-matrix least-squares on F^2
Data / restraints / parameters	8272 / 0 / 574	5865 / 33 / 343	3804 / 0 / 175
GOF / F^2	1.019	0.846	0.859
Final *R* indices [$I>2\sigma(I)$]	$R1 = 0.0348$, $wR2 = 0.0706$	$R1 = 0.0795$, $wR2 = 0.1877$	$R1 = 0.0345$, $wR2 = 0.1032$
R indices (all data)	$R1 = 0.0571$, $wR2 = 0.0770$	$R1 = 0.1278$, $wR2 = 0.2027$	$R1 = 0.0493$, $wR2 = 0.1144$
Largest diff. peak and hole (e Å^{-3})	274 and -0.551	0.495 and -1.076	0.393 and –0.591

Table 12 Key X-ray Parameters, Refinement and Results for 8 and 9

	(TTP)Zr(CH$_2$Ph)$_3$ (8)	**(TTP*)Zr(CH$_2$Ph)$_2$ (9)**
Empirical formula	$C_{40}H_{47}N_2Zr$	$C_{33}H_{34}N_2Zr$
Formula weight	647.02	549.84
Temperature (K)	173(2)	173(2)
Wavelength (Å)	0.71073	0.71073
Crystal system	Monoclinic	Triclinic
Space group	C2/c	$P\bar{1}$
Cell		
a (Å)	40.287(8)	10.167(2)
b (Å)	9.191(2)	11.547(2)
c (Å)	20.566(4)	13.192(3)
α (°)	90	87.81(3)
β (°)	117.27(3)	72.59(3)
χ (°)	90	69.06(3)
Volume (Å^3)	6769(2)	1376.0(5)
Z	8	2
d (calc.) (Mg/m^3)	1.270	1.327
Abs. Coef. (mm^{-1})	0.354	0.423
F(000)	2728	572
Crystal size (mm)	0.2 x 0.2 x 0.2	0.2 x 0.2 x 0.25
2*θ* range (°)	1.98 to 28.40	1.62 to 28.32
Index ranges	$-53 <= h <= 39$ $-11 <= k <= 12$ $-25 <= l <= 26$	$-13 <= h <= 13$ $-15 <= k <= 14$ $-17 <= l <= 17$
Reflections collected	19559	16390
Independent reflections	7797 [*R*(int) = 0.0504]	6494 [*R*(int) = 0.0300]
Refinement method	Full-matrix least-squares on F^2	Full-matrix least-squares on F^2
Data / restraints / parameters	7796 / 0 / 556	6494 / 459 / 409
GOF / F^2	1.000	1.009
Final *R* indices [$I>2\sigma(I)$]	*R*1 = 0.0446, *wR*2 = 0.0822	*R*1 = 0.0305, *wR*2 = 0.0708
R indices (all data)	*R*1 = 0.0811, *wR*2 = 0.0939	*R*1 = 0.0416, *wR*2 = 0.0741
Largest diff. peak and hole (e Å^{-3})	0.345 and –0.635	0.265 and –0.444

Table 13 Key X-ray Parameters, Refinement and Results for 10, 11 and 13

	$(TTP)Zr(NMe_2)_3$ (10)	**$(TTP)Ti(NMe_2)_3$ (11)**	**$(TP)_2Zr(NMe_2)_2$ (13)**
Empirical formula	$C_{25}H_{39}N_5Zr$	$C_{25}H_{39}N_5Ti$	$C_{28}H_{40}N_4O_2Zr$
Formula weight	500.83	457.51	555.86
Temperature (K)	173(2)	173(2)	173(2)
Wavelength (Å)	0.71073	0.71073	0.71073
Crystal system	Triclinic	Triclinic	Monoclinic
Space group	$P\bar{1}$	$P\bar{1}$	$P2_1/c$
Cell			
a (Å)	8.669(2)	8.69720(10)	18.272(4)
b (Å)	10.385(2)	10.51620(10)	9.102(2)
c (Å)	15.874(3)	15.53630(10)	17.200(3)
α (°)	102.19(3)	102.53	
β (°)	92.92(3)	93.59	98.15(3)
χ (°)	101.28(3)	102.5190(10)	
Volume ($Å^3$)	1363.5(5)	1345.12(2)	2831.5(1)
Z	2	2	4
d (calc.) (Mg/m^3)	1.220	1.130	1.304
Abs. coef. (mm^{-1})	0.422	0.337	0.418
F(000)	528	492	1168
Crystal size (mm)	0.20 x 0.20 x 0.25	0.2 x 0.2 x 0.15	0.24 × 0.22 × 0.20
2θ range (°)	2.05 to 28.34	1.35 to 28.23	2.25 to 28.34
Index ranges	$-11 <= h <= 11$ $-13 <= k <= 13$ $-19 <= l <= 20$	-11 <= h <= 11 -13 <= k <= 13 -20 <= l <= 20	$-23 \leq h \leq 23$ $5 \leq k \leq 12$ $20 \leq l \leq 22$
Reflections collected	11671	13940	14661
Independent reflections	6153 [*R*(int) = 0.0905]	6100 [*R*(int) = 0.0196]	6399 [*R*(int) = 0.0752]
Refinement method	Full-matrix least-squares on F^2	Full-matrix least-squares on F^2	Full-matrix least-squares on F^2
Data / restraints / parameters	6153 / 0 / 280	6100 / 0 / 436	6399 / 0 / 316
GOF / F^2	0.300	0.921	0.987
Final *R* indices [$I>2\sigma(I)$]	$R1 = 0.0575$, $wR2 = 0.1382$	$R1 = 0.0359$, $wR2 = 0.1121$	$R1 = 0.0771$ $wR2 = 0.1613$
R indices (all data)	$R1 = 0.0969$, $wR2 = 0.1527$	$R1 = 0.0466$, $wR2 = 0.1205$	$R1 = 0.1500$ $wR2 = 0.1958$
Largest diff. peak and hole (e $Å^{-3}$)	0.379 and –0.608	0.254 and –0.327	0.496 and -0.652

Table 14 Key X-ray Parameters, Refinement and Results for 14

	(DDP)ZrCl(NMe$_2$)$_2$ (14)
Empirical formula	[$C_{33}H_{53}ClN_4Zr$]$_2$
Formula weight	1264.93
Temperature (K)	173(2)
Wavelength (Å)	0.71073
Crystal system	Triclinic
Space group	$P\overline{1}$
Cell	
a (Å)	12.31060(10)
b (Å)	16.8085(3)
c (Å)	17.5560(3)
α (°)	87.0030(10)
β (°)	76.07
χ (°)	77.9970(10)
Volume (Å^3)	3448.82(9)
Z	2
d (calc.) (Mg/m^3)	1.218
Abs. coef. (mm^{-1})	0.422
F(000)	1344
Crystal size (mm)	0.18 x 0.15 x 0.08
2θ range (°)	1.72 to 28.30
Index ranges	$-16 <= h <= 12$ $-22 <= k <= 21$ $-23 <= l <= 22$
Reflections collected	25293
Independent reflections	15168 [*R*(int) = 0.0293]
Refinement method	Full-matrix least-squares on F^2
Data / restraints / parameters	15168 / 0 / 703
GOF / F^2	0.836
Final *R* indices [I>2σ(I)]	$R1 = 0.0424$, $wR2 = 0.1138$
R indices (all data)	$R1 = 0.0696$, $wR2 = 0.1314$
Largest diff. peak and hole (e Å^{-3})	0.503 and -0.506

REFERENCES

1. (a) Fabro, S. I. In *Biochemical Basis of Teragenesis*; Juchau, M. R., Ed; Elsevier: Amsterdam, **1981**; p 159. (b) Borman, S. *Chem. Eng. News* **1990**, *68*, 9. (c) De Camp, W. H. *Chirality* **1989**, *1*, 2.

2. Crout, D. H. G.; Christen, M. In *Modern Synthetic Methods*; Scheffold, R., Ed.; Springer-Verlag: New York, **1989**; Vol. 5, p 1 and references therein.

3. Brunner, H. In *Topics in Stereochemistry*; Eliel, E. L.; Wilen, S. H., Eds.; Wiley & Sons: New York, **1988**; Vol 18, p 129 and references therein.

4. Noyori, R.; Kitamura, M. In *Modern Synthetic Methods*; Scheffold, R., Ed.; Springer-Verlag: New York, **1989**; Vol 5, p 115 and references therein.

5. Klunder, A. J.; Huizuga, W. B.; Hulshof, A. J. M.; Zwanenburg, B. *Tet. Lett.* **1986**, *27*, 2543.

6. Gais, H. J.; Lukas, K. L.; Bull, W. A.; Braun, S.; Linder, H. J. *Liebigs Ann. Chem.* **1986**, 687.

7. Nugent, W. A.; RajanBabu, T. V.; Burk, M. J. *Science* **1993**, *259*, 479.

8. Jacobsen, E. N. In *Cataytic Asymmetric Synthesis*; Ojima, I., Ed.; VCH: New York, **1993**; p 176

9. Tokunaga, M.; Larrow, J. F.; Kakiuchi, F.; Jacobsen, E. N. *Science* **1997**, *277*, 936.

10. Palucki, M.; Finney, N. S.; Pospisil, P. J.; Guler, M. L.; Ishida T.; Jacobsen, E. N. *J. Am. Chem. Soc.* **1998**, *120*, 948.

11. Cotton, F. A.; Wilkinson, G. *Advanced Inorganic Chemistry 5th Ed.*; John Wiley & Sons: New York, **1988**, 203, 1237, 1245, 1256.

12. Odian, G. *Principles of Polymerization*; John Wiley & Sons: New York, **1991**.

13. (a) Natta, G.; Pino, P.; Corrandini, P.; Danusso, F.; Mantica, G.; Moraglio, G. *J. Am. Chem. Soc.* **1955**, *77*, 1708. (b) Natta, G. *Angew. Chem.* **1956**, *68*, 3930. (c) Natta, G. *Angew. Chem.* **1964**, *76*, 553.

14. (a) Taube, R.; Krukowka, L. *J. Organomet. Chem.* **1988**, *347*, C9. (b) Bochmann, M.; Jaggar, A. J. *J. Organomet. Chem.* **1992**, *424*, C5.

15. (a) Gassman, P.G.; Callstrom, M. R. *J. Am. Chem. Soc.* **1987**, *109*, 7875. (b) Eisch, J. J.; Pombrik, S. I.; Zheng, G. X. *Organometallics* **1993**, *12*, 3856. (c) Bochmann, M.; Jagger, A. *J. Organomet. Chem.* **1992**, *424*, C5.

16. Ewen, J. A.; *J. Am. Chem. Soc.* **1984**, *106*, 6355.

17. Grassi, A.; Zambelli, A.; Resconi, L.; Albizzati, E.; Mazzocchi, R. *Macromolecules* **1988**, *21*, 617.

18. Mohring, P. C.; Conville, N. J. *J. Organomet. Chem.* **1994**, *479*, 1.

19. Feldman, J.; McLain, S. J.; Parthasarthy, A.; Marshall, W. J; Calabrese, J. C.; Arthur, S. D. *Organometallics* **1997**, *16*, 1514.

20. Johnson, L. K.; Killian, C. M.; Brookhart, M. *J. Am. Chem. Soc.* **1995**, *117*, 6414.

21. Johnson, L. K.; Mecking, S.; Brookhart, M. *J. Am. Chem. Soc.* **1996**, *118*, 267.

22. (a) Rix, F.; Brookhart, M. *J. Am. Chem. Soc.* **1995**, *117*, 1137. (b) Peuckert, M.; Keim, W. *Organometallics* **1983**, *2*, 594. (c) Wilke, G. *Angew. Chem. Int. Ed. Engl.* **1988**, *27*, 185.

23. (a) Holm, R. H.; Parks, J. E. *Inorg. Chem.* **1968**, *7*, 1408. (b) McGeachin, S. G. *Can. J. Chem.* **1968**, *46*, 1903.

24. Cheng, M.; Lobkovsky, E. B.; Coates, G. W. *J. Am. Chem. Soc.* **1998**, *120*, 11018.

25. Qian, B.; Ward, D. L.; Smith III, M. R. *Organometallics* **1998**, *17*, 3070.

26. Radzewich, C. E.; Coles, M. P.; Jordan, R. F. *J. Am. Chem. Soc.* **1998**, *120*, 9384.

27. Hitchcock, P. B.; Lappert, M. F.; Liu, D. *Chem. Comm.* **1994**, 2637.

28. Rahim, M; Taylor, N. J.; Xin, S; Collins, S. *Organometallics* **1998**, *17*, 1315.

29. Kim, W. K.; Fevola, M. J.; Liable-Sands, L.M.; Rheingold, A. L.; Theopold, K. H. *Organometallics* **1998**, *17*, 4541.

30. Martin, A.; Uhrhammer, R; Garderner, T. G.; Jordan, R. F.; Rogers, R. D. *Organometallics*, **1998**, *17*, 382.

31. (a) Floriani, C.; Curli, S.; Chiesi-Villia, A.; Gustini, C. *Angew Chem., Int. Ed. Engl.* **1987**, *26*, 70. (b) Giannini, L.; Solari, E.; DeAngelis, S.; Ward, T. R.; Floriani, C.; Chiesi-Villia, A.; Rizzoli, C. *J. Am. Chem. Soc.* **1995**, *117*, 5801. (c)

Black, D. G.; Swenson, D. C.; Jordan, R. F.; Rogers, R. D. *Organometallics* **1995**, *14*, 3539. (d) Black, D. G.; Jordan, R. F.; Rogers, R. D. *Inorg. Chem.* **1997**, *36*, 103.

32. Scollard, J. D.; McConville, D. H. *J. Am. Chem. Soc.* **1996**, *118*, 10008.

33. Scollard, J. D.; McConville, D. H.; Payne, N. C.; Vittal, J. J. *Macromolecules*, **1996**, *29*, 5241.

34. (a) Scollard, J. D.; McConville, D. H.; Vittal, J. J. Organometallics 1997, 16, 4415. (b) Scollard, J. D.; McConville, D. H.; Vittal, J. J. Organometallics 1995, 14, 5478.

35. (a) Zhou, Y.; Richeson, D. S. *Inorg. Chem.* **1996**, *35*, 1423. (b) Zhou, Y.; Richeson, D. S. *Inorg. Chem.* **1996**, *35*, 2448. (c) Zhou, Y.; Richeson, D. S. *J. Am. Chem. Soc.* **1996**, *118*, 10850. (d) Zhou, Y.; Richeson, D. S. *Inorg. Chem.* **1997**, *36*, 501. (e) Foley, S. R.; Richeson, D. S. *J. Am. Chem. Soc.* **1997**, *119*, 10359.

36. Cragg-Hine, I.; Davidson, M. G.; Mair, F. S.; Raithby, P. R.; Snaith, R. *J. Chem. Soc., Dalton Trans.* **1993**, 2423.

37. Duchateau, R.; van Wee, C. T.; Meetsma, A.; van Duijnen, P. T.; Teuben, J. H. *Organometallics*, **1996**, *15*, 2279.

38. Herskovics-Korine, D.; Eisen, M. S. *J. Organomet. Chem.* **1995**, *503*, 307.

39. For examples, see references 1-3 contained in (33)

40. Flores, J. C.; Chien, J. C. W.; Rausch, M. D. *Organometallics* **1995**, *14*, 1827.

41. Hagadorn, J. R.; Arnold, J. *J. Chem. Soc., Dalton Trans.* **1997** 3087.

42. Littke, A.; Sleiman, N.; Bensimon, C.; Richeson, D. S.; Yap, G. P. A.; Brown, S. J. *Organometallics* **1998**, *17*, 446.

43. Warren, T. H.; Schrock, R. R.; Davis, W. M. *Organometallics* **1996**, *15*, 562.

44. Chisholm, M. H.; Eilerts, N. W. *Chem. Comm.* **1996**, 853.

45. Kakaliou, L. Michigan State University, unpublished results.

46. (a) Bailar, J. C. *J. Inorg. Nucl. Chem.* **1958**, *8*, 165. (b) Wentworth, R. A. D. *Coord. Chem. Rev.* **1972**, *9*, 171. (c) Fleischer, E. B.; Gebala, A. E.; Swift, D. R.; Tasker, P. A. *Inorg. Chem.* **1972**, *11*, 2775. (d) Chruchill, M. R.; Reis, A. H.

Inorg. Chem. **1972,** *11,* 1811. (e) Vanquickenborne, L. G.; Pierloot, K. *Inorg. Chem.* **1981**, *20*, 3673. (f) Darensberg, D. J.; Kump, R. L. *Inorg. Chem.* **1984**, *23*, 2993.

47. Yin, M. Michigan State University, unpublished results.

48. Motry, D. Michigan State University, unpublished results.

49. Davies, G. R, Jarvis, J. A. J, Kilbourn, B. T., Pioli, A. J. P. *Chem. Comm.* **1971,** 677.

50. Qian, B. Michigan State University, unpublished results.

51. Weingarten, H.; Miles, M. G. *J. Org. Chem.* **1968,** *33*, 1506.

52. Baek, S. Michigan State University, unpublished results.

53. Nelsen, S. F.; Landis, R. T. *J. Am. Chem. Soc.* **1973,** *95*, 26.

54. Kabalka, G. W.; Stastry, U.; Stastry, K. A. R.; Knapp, F. F.; Srivastava, P. C. *J. Organomet. Chem.* **1983**, *3*, 259.

55. Wallow, T. I.; Novak, B. M. *J. Organomet. Chem.* **1994,** *59*, 5034.

56. Manzer, L. E. *Inorg. Syntheses* **1982,** *21*, 135.

57. Zucchini, U.; Albizzati, E.; Giannini, U. *J. Organomet. Chem.* **1971,** *26*, 357.

58 Bradley, D. C.; Thomas, I. M. *J. Chem. Soc.* **1960,** 3857.

59. Naiini, A. A.; Ringrose, S. L.; Su, Y.; Jacobson, R. A.; Verkade, J. G. *Inorg. Chem.* **1993,** *32*, 1290.